

---

# Variational Beam Search for Learning with Distribution Shifts

---

Aodong Li<sup>1</sup> Alex Boyd<sup>2</sup> Padhraic Smyth<sup>1,2</sup> Stephan Mandt<sup>1,2</sup>

## Abstract

We consider the problem of online learning in the presence of sudden distribution shifts as frequently encountered in applications such as autonomous navigation. Distribution shifts require constant performance monitoring and re-training. They may also be hard to detect and can lead to a slow but steady degradation in model performance. To address this problem we propose a new Bayesian meta-algorithm that can both (i) make inferences about subtle distribution shifts based on minimal sequential observations and (ii) accordingly adapt a model in an online fashion. The approach uses beam search over multiple change point hypotheses to perform inference in a hierarchical sequential latent variable modeling framework. Our proposed approach is model-agnostic, applicable to both supervised and unsupervised learning, and yields significant improvements over state-of-the-art Bayesian online learning approaches.

## 1. Introduction

Deployed machine learning systems are often faced with the problem of distribution shift, where the new data that the model processes is systematically different from the data the system was trained on (Zech et al., 2018; Ovadia et al., 2019). Furthermore, a shift can happen anytime after deployment, unbeknownst to the users, with dramatic consequences for systems such as self-driving cars, robots, and trading algorithms, among many other examples.

Updating a deployed model on new, representative data can help mitigate these issues, as well as improve general performance in most cases. This task is commonly referred to as *online* or *incremental learning*. A particular variant of online learning that focuses on adapting models to new or novel data (in either features and/or outputs) over time is known as *continual learning*. Approaches developed for this

task typically focus on mitigating the degradation of performance over earlier data, often referred to as *catastrophic forgetting*. For instance, variational continual learning (VCL) (Nguyen et al., 2018) is a popular framework designed to prevent forgetting by drawing on Bayesian online learning.

In contrast to the usual continual learning paradigm where the data distribution is considered stationary, we consider time-varying data distributions. While VCL and other Bayesian solutions are typically robust to catastrophic forgetting, we show that they suffer from an opposite problem for non-stationary data that we define as *catastrophic remembering*. When a Bayesian model is continually trained, its posterior distribution becomes progressively more and more confident as more data is used to inform it. Given enough data, the model’s prior distribution (i.e. previous posterior distribution) will be too confident to adequately adapt to new data that has been affected by a distributional shift.

In this paper, we propose a robust approach that copes with the problems of both catastrophic forgetting *and* catastrophic remembering. It is based on two assumptions: first, distribution shifts occur irregularly and have to be inferred from the data, and second, the model requires not only a good mechanism to aggregate data, but also the ability to partially forget information that has become obsolete. To solve both problems, we still use a Bayesian framework for online learning (i.e. letting a previous posterior distribution be used as the next prior); however, before combining the previously learned posterior with new data evidence, we introduce an intermediate step. This step allows the model to decide between two actions to take: broaden the previous posterior to reduce the model’s confidence and provide more “room” for new information, or remain in the same state (i.e. retain the unchanged, previous posterior as the new prior).

We propose a mechanism for enabling this decision using a “spike and slab” prior that influences how likely the model is to detect a distributional shift and in what ways it will broaden the posterior distribution upon detection. We further augment this decision process by introducing *variational beam search*, a new inference scheme that allows the model to consider multiple different hypothetical sequences of detected distributional shifts (or lack thereof).

Our experiments show the many advantages of our proposed approach. First, because our method can both remember

---

<sup>1</sup>Department of Computer Science, University of California, Irvine <sup>2</sup>Department of Statistics, University of California, Irvine. Correspondence to: Aodong Li <aodongl1@uci.edu>.

and also partially forget, we show that it is better suited to online learning setups that involve a long stream of data with multiple distributional shifts that occur at unknown times. Second, our beam search approach consistently outperforms a simple, greedy variant because it can better reason in hindsight. Our main contributions are as follows:

- We study continual learning on non-stationary data distributions and provide intuition as to why current Bayesian approaches fail, namely from a lack of ability to partially forget information. We point out that catastrophic remembering and forgetting are two equally harmful scenarios in this setup.
- We present a new approach to joint change point detection and continual learning in a hierarchical Bayesian framework. Assuming that distribution shifts happen at unknown times, we propose a new spike and slab dynamics prior coupled with a novel filtering scheme. This scheme can be further refined with beam search, resulting in a novel structured variational approximation.
- We perform experiments for supervised learning with Bayesian neural networks and linear regression using both real data with artificially induced shifts over time and real data that naturally contain distribution shifts. We also perform unsupervised learning experiments for analyzing semantic changes over time in language. Our approach both leads to more compact and interpretable latent structure as well as significantly improved performance in the supervised experiments.

Our paper is structured as follows: we review related work in Section 2, introduce our methods in Section 3, report our experiments in Section 4, and draw conclusions in Section 5.

## 2. Related Work

Our paper connects to related work in continual learning, change detection, and switching linear dynamical systems.

**Continual Learning** Goodfellow et al. (2014) first empirically studied the effect of catastrophic forgetting in deep learning and suggested dropout as a solution. Shin et al. (2017) proposed non-Bayesian continual learning with replay which used GANs to restore old data points. Kirkpatrick et al. (2017) proposed elastic weight consolidation, which updates parameters while having a quadratic regularizer centered around the old parameter values for the new task. Nguyen et al. (2018) first proposed variational continual learning, which forms the basis of our approach. The scheme was generalized by Farquhar & Gal (2018). Schwarz et al. (2018) provided a recent overview and benchmarks.

Similar to Aljundi et al. (2019) and Kurle et al. (2020), we consider a version of continual learning on non-stationary data. Like other related works that use Gaussian processes (Titsias et al., 2019), Dirichlet processes (Lee et al., 2020), and expandable representation learning (Rao et al., 2019), we assume that distribution shifts occur irregularly.

**Change Point Models** Our approach relies on jointly inferring changes in the data distribution while carrying out Bayesian parameter updates; as such, our change detection operates in a high-dimensional parameter space. This is in contrast to classical works on change detection from the statistics literature that typically considers one-dimensional (or low-dimensional) sequences. Fearnhead (2005) proposed change detection in the context of regression and generalized it to online inference (Fearnhead & Liu, 2007). Adams & MacKay (2007) described a Bayesian *online* change point detection scheme based on conditional conjugacy assumptions for one-dimensional sequences. Xuan & Murphy (2007) introduced a change point detection algorithm for multivariate time series. Xie et al. (2012) described a change point algorithm for multivariate time series in a manifold learning framework. Titsias et al. (2020) proposed change detection to detect distribution shifts in sequences based on low-dimensional summary statistics, such as a loss function. In contrast to all these works, our approach jointly detects and responds to changes in high dimensions.

**Switching Linear Dynamical Systems** Linderman et al. (2017) considered *recurrent* switching linear dynamical systems, relying on Bayesian conjugacy and closed-form message passing updates. Becker-Ehmck et al. (2019) proposed a variational Bayes filtering framework for switching linear dynamical systems. Murphy (2012) and Barber (2012) developed an inference method using a Gaussian sum filter.

Bracegirdle & Barber (2011) introduce a *reset* variable that sets the continuous latent variable to an unconditional prior—which is similar to our own work. Our tempered broadening can be seen as a partial reset, augmented with beam search.

## 3. Methods

**Overview** Section 3.1 introduces the setup under consideration. Section 3.2 introduces a novel conditional posterior tempering mechanism for inferring and mitigating distribution shifts. Inference in these models is introduced in Section 3.3. Finally, we introduce the beam search extension in Section 3.4.

### 3.1. Problem Setup and Discussion

We consider a stream of data that arrives in batches (also referred to as “tasks”)  $\mathbf{x}_t$  at discrete times  $t$ . For supervised

setups, we consider pairs of features and targets  $(\mathbf{x}_t, \mathbf{y}_t)$ , where the task is to model  $p(\mathbf{y}_t|\mathbf{x}_t)$ . For notational simplicity we focus on the unsupervised case, where the task is to model  $p(\mathbf{x}_t)$  using a model  $p(\mathbf{x}_t|\mathbf{z}_t)$  with parameters  $\mathbf{z}_t$  that we would like to optimally tune to each new batch<sup>1</sup>.

We furthermore assume that while the  $\mathbf{x}_t$  are i.i.d. within batches, they are not i.i.d. across batches, but rather come from a time-varying distribution  $p_t(\mathbf{x}_t)$  (or  $p_t(\mathbf{x}_t, \mathbf{y}_t)$  in the supervised cases) which is subject to distribution shifts. We assume that these distribution shifts occur instantaneously (as opposed to gradually) and at unknown times, i.e., a change may (or may not) occur with each batch  $t$  and (if it occurs) will persist until the next change. The challenge is to optimally adapt the parameters  $\mathbf{z}_t$  to each new task while borrowing statistical strength from previous tasks.

**Variational Continual Learning** The basis of our approach is the insight that for sequential data, one can use a Bayesian model’s posterior at time  $t - 1$  as a prior for the next task at time  $t$ . Since typically the posterior is not available in closed-form, we must use approximate inference. And since Markov chain Monte Carlo methods can be impractical for highly-parametrized machine learning models such as deep networks, it is natural to use a variational posterior  $q_{t-1}(\mathbf{z}_t)$  instead. This leads to a sequence of variational inference tasks (Zhang et al., 2018) known as variational continual learning (VCL) (Nguyen et al., 2018):

$$q_t(\mathbf{z}_t) = \arg \max_{q(\mathbf{z}_t) \in Q} \mathbb{E}_q[\log p(\mathbf{x}_t|\mathbf{z}_t)] - \text{KL}(q(\mathbf{z}_t)||q_{t-1}(\mathbf{z}_t)), \quad (1)$$

where  $Q$  is the family of potential approximate posterior distributions (i.e. normal distributions).

Eq. 1 is known as the evidence lower bound (ELBO) in variational inference (Jordan et al., 1999; Zhang et al., 2018); for every new task it is optimized until convergence. Note that in its original formulation, the goal of VCL is to train a model that performs well cumulatively on *all* the learning tasks previously encountered (Nguyen et al., 2018), as opposed to just the most recent task as studied in this paper.

**Catastrophic Remembering** While continual learning mainly addresses catastrophic forgetting, where a model loses in performance on the tasks previously encountered, we address the opposite effect: catastrophic remembering. Here, a model becomes overconfident with time and loses its ability to adapt to distribution shifts. On non-stationary data, such catastrophic remembering is caused by an overconfident posterior. To explain this effect, we note that a posterior’s variance shrinks as it encounters more data. Assume

<sup>1</sup>In supervised setups, we consider a conditional model  $p(\mathbf{y}_t|\mathbf{z}_t, \mathbf{x}_t)$  with features  $\mathbf{x}_t$  and targets  $\mathbf{y}_t$ .

that after a long sequence of updates, the posterior  $q_{t-1}(\mathbf{z}_t)$  can be well-approximated by a point mass  $\delta(\mathbf{z}_t - \mathbf{z}_0)$  centered around some parameter  $\mathbf{z}_0$ . In this case, any new data evidence  $p(\mathbf{x}_t|\mathbf{z}_t)$  will have a diminishing effect on the next posterior  $q_t(\mathbf{z}_t)$  as  $q_t(\mathbf{z}_t) \propto p(\mathbf{x}_t|\mathbf{z}_t)\delta(\mathbf{z}_t - \mathbf{z}_0) \approx q_{t-1}(\mathbf{z}_t)$ , in other words, the strong prior over-rides the new data even though the training data that lead to it may have become obsolete due to a distribution shift. We visualize this catastrophic remembering effect through an online linear regression (Supplement E).

### 3.2. Resetting the Prior by Tempering

In order to combat catastrophic remembering, the posterior in Eq. 1 needs to be broadened before it can be used as a prior for the next task. We therefore consider a generalized variational filtering scheme of the following kind:

$$q_t(\mathbf{z}_t) = \arg \max_{q(\mathbf{z}_t) \in Q} \mathbb{E}_q[\log p(\mathbf{x}_t|\mathbf{z}_t)] - \text{KL}(q(\mathbf{z}_t)||\mathcal{F}(q_{t-1})(\mathbf{z}_t)). \quad (2)$$

We call  $\mathcal{F}$  the *posterior broadening functional*; its role is to broaden the posterior before using it as a prior. This erases learned information to free-up model capacity to adjust to the new data distribution.

We consider *tempering*, which amounts to raising prior to the power  $\beta$  and renormalizing, i.e.  $\mathcal{F}_\beta(q_{t-1})(\mathbf{z}_t) \propto q_{t-1}(\mathbf{z}_t)^\beta$  for  $0 < \beta \leq 1$ . For a Gaussian  $q$  with diagonal variances  $\sigma_i^2$  in dimension  $\mathbf{z}_i$ , tempering removes an equal amount of information in each dimension,  $H_i = \frac{1}{2} \log(2\pi e \sigma_i^2 / \beta) = \frac{1}{2} \log(2\pi e \sigma_i^2) - \frac{1}{2} \log \beta$ . See Supplement B for more details on this choice.

**Conditional Tempering** If distribution shifts happened at a predictable and constant rate then we would simply need to tune the parameter  $\beta$  to the expected rate of change (with a small  $\beta$  for a high change rate and  $\beta = 1$  for no expected change). In reality, however, distribution shifts can be of varying strength, irregular, and *unobserved*. We therefore propose to model the distribution shift at time  $t$  with a binary latent variable  $s_t$ , with  $s_t = 0$  for no change occurring, and  $s_t = 1$  indicating a shift. For  $s_t = 1$ , we temper the posterior and use it as the new prior. If no change occurs, we just proceed with the previous posterior as the new prior. This gives rise to the following conditional prior:

$$p_\beta(\mathbf{z}_t|s_t) = \begin{cases} q_{t-1}(\mathbf{z}_t) & \text{for } s_t = 0 \\ q_{t-1}^\beta(\mathbf{z}_t) & \text{for } s_t = 1 \end{cases}, \quad (3)$$

which corresponds to the spike and slab prior where “spike” sets  $s_t = 0$  and “slab” sets  $s_t = 1$ . We defined the tempered approximate posterior at time  $t - 1$  as  $q_{t-1}^\beta(\mathbf{z}_t) = \frac{(q_{t-1}(\mathbf{z}_t))^\beta}{\int (q_{t-1}(\mathbf{z}_t))^\beta d\mathbf{z}_t}$ . (Note that  $q^\beta$  has a closed-form expression

for a Gaussian  $q$ .) The conditional tempering approach leads to the following online inference scheme:

$$q_t(\mathbf{z}_t | s_t) = \arg \max_{q(\mathbf{z}_t | s_t) \in \mathcal{Q}} \mathcal{L}(q | s_t), \quad (4)$$

$$\mathcal{L}(q | s_t) := \mathbb{E}_q[\log p(\mathbf{x}_t | \mathbf{z}_t)] - \text{KL}(q(\mathbf{z}_t | s_t) || p_\beta(\mathbf{z}_t | s_t)).$$

This involves a joint variational distribution  $q(\mathbf{z}_t | s_t)$  over the latents  $\mathbf{z}_t$  and change variable  $s_t$ . We place a Bernoulli prior  $p(s_t)$  on the change variables. As described below, we jointly infer  $\mathbf{z}_t$  and the change variables  $s_t$  from data.

### 3.3. Bayesian Reasoning over Distribution Shifts

According to our assumptions, the distribution shifts occur at discrete times and are unobserved. Therefore, both  $\mathbf{z}_t$  and  $s_t$  have to be inferred from data. For simplicity, we first describe a hypothetical exact inference scheme and then describe corresponding setup for variational inference (with exact derivations provided in Supplement A).

**Exact Inference** We first formally define the (intractable) marginal likelihood over data given the change variable  $s_t$ ,

$$p_\beta(\mathbf{x}_t | s_t) = \int p(\mathbf{x}_t | \mathbf{z}_t) p_\beta(\mathbf{z}_t | s_t) d\mathbf{z}_t. \quad (5)$$

The exact posterior over  $s_t$  is again a Bernoulli  $p_\beta(s_t | \mathbf{x}_t) = \text{Bern}(s_t; m)$  with parameter

$$m = \sigma \left( \log \frac{p_\beta(\mathbf{x}_t | s_t = 1) p(s_t = 1)}{p_\beta(\mathbf{x}_t | s_t = 0) p(s_t = 0)} \right) \stackrel{\text{Eq. 3}}{=} \sigma \left( \log \frac{\int p(\mathbf{x}_t | \mathbf{z}_t) q_{t-1}^\beta(\mathbf{z}_t) d\mathbf{z}_t}{\int p(\mathbf{x}_t | \mathbf{z}_t) q_{t-1}(\mathbf{z}_t) d\mathbf{z}_t} + \xi_0 \right), \quad (6)$$

where  $\sigma$  is the sigmoid function and  $\xi_0 = \log p(s_t = 1) - \log p(s_t = 0)$  are the log-odds of the prior  $p(s_t)$ . This specifies the posterior over  $s_t$ .

Eq. 6 has a simple interpretation as a likelihood ratio test: a change is more or less likely depending on whether or not the observations  $\mathbf{x}_t$  are better explained under the assumption of the tempered prior distribution  $q_{t-1}^\beta(\mathbf{z}_t)$ , in other words, a partial reset of previously learned information.

**Structured Variational Inference** Unfortunately, the marginal in Eq. 5 is not available, leaving Eq. 6 intractable to evaluate. However, we can follow a structured variational inference approach (Wainwright & Jordan, 2008; Hoffman & Blei, 2015; Zhang et al., 2018), defining a joint variational distribution  $q(\mathbf{z}_t, s_t) = q(s_t)q(\mathbf{z}_t | s_t)$ .

By definition, the conditional distributions  $q(\mathbf{z}_t | s_t)$  are solutions to the optimization problem in Eq. 4. One may wonder how the exact inference scheme for  $s_t$  is modified in the structured variational inference scenario. In Supplement A,

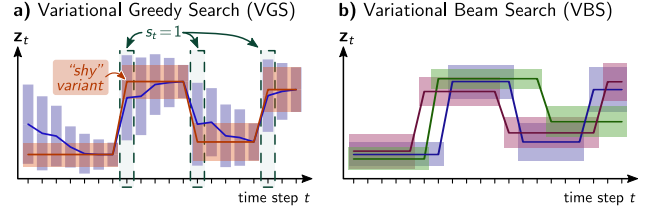


Figure 1. Sparse inference via greedy search (left) and variational beam search (right). Solid lines indicate fitted mean  $\mu_t$  over time steps  $t$  with boxes representing  $\pm 1\sigma$  error bars. Please see more information about the pictured “shy” variant in Supplement C.

we derive the following closed-form update equation for  $q(s_t)$  that bears strong similarities to Eq. 6. Since the conditional ELBO in Eq. 4 is a lower bound to the logarithm of the marginal likelihood in Eq. 5, we can use the former as a proxy of the latter, resulting in the update

$$q^*(s_t) = \text{Bern}(s_t; m); \quad (7)$$

$$m = \sigma \left( \frac{1}{T} \mathcal{L}(q | s_t = 1) - \frac{1}{T} \mathcal{L}(q | s_t = 0) + \xi_0 \right).$$

Above, we introduced a parameter  $T \geq 1$  (not to be confused with  $\beta$ ) to optionally downweigh the data evidence relative to the prior (see experiments section). As a result of Eq. 7, we obtain the marginal distribution over latent variables  $q(\mathbf{z}_t)$  at time  $t$  as a binary mixture with mixture weights  $q(s_t = 0) = m$  and  $q(s_t = 1) = 1 - m$ :

$$q_t(\mathbf{z}_t) = m q(\mathbf{z}_t | s_t = 0) + (1 - m) q(\mathbf{z}_t | s_t = 1). \quad (8)$$

**Exponential Branching** We note that while we had originally started with a Gaussian variational posterior  $q_{t-1}(\mathbf{z}_t)$  at the previous time, our inference scheme resulted in  $q_t(\mathbf{z}_t)$  being a mixture of two Gaussians:<sup>2</sup> the inference scheme branches over two alternative hypotheses. When we iterate, we encounter an exponential branching of possibilities, or *hypotheses* over possible sequences of regime shifts. To still be able to carry out the filtering scheme efficiently, we need a truncation scheme, e.g., approximate the bimodal marginal distribution by a unimodal one. The next section will discuss several methods to achieve this goal.

### 3.4. Online Inference and Variational Beam Search

While the previous subsections have focused on a single update, we now investigate the possibility of doing multiple updates in a row. This amounts to working out a truncation scheme to restrict the variational posterior to be a unimodal Gaussian (or, a mixture of fixed size) at every time step.

**Variational Greedy Search** In the simplest “greedy” setup, we train the model in an online fashion by iterat-

<sup>2</sup>See also Fig. 6 in Supplement C.

ing over time steps  $t$ . For each  $t$ , we update a *truncated* variational distribution via the following three steps:

1. Compute the conditional prior  $p_\beta(\mathbf{z}_t|s_t)$  (Eq. 3) based on  $q_{t-1}$  and optimize the conditional ELBO (Eq. 4) for both  $s_t = 0$  and  $s_t = 1$ . This results in the optimized variational distributions  $q(\mathbf{z}_t|s_t = 0)$  and  $q(\mathbf{z}_t|s_t = 1)$ .
2. Compute the binary mixture weights  $m$  and  $(1 - m)$  using Eq. 7, resulting in  $q_t(\mathbf{z}_t) = m q(\mathbf{z}_t|s_t = 0) + (1 - m)q(\mathbf{z}_t|s_t = 1)$  (Eq. 8).
3. Truncate  $q_t(\mathbf{z}_t)$  to a uni-modal distribution to avoid branching by projecting the mixture of two components on the more probable one (i.e., make a ‘‘hard’’ decision with a threshold of  $\frac{1}{2}$ ).

The above filtering algorithm iteratively updates the variational distribution over  $\mathbf{z}_t$  each time it observes new data  $\mathbf{x}_t$ . In the version of variational greedy search (VGS) discussed above, the approach decides immediately, i.e., before observing subsequent data points, whether a change in  $\mathbf{z}_t$  has occurred or not in step 3. (Please note the decision is irrelevant to history, as opposed to the beam search described below.) VGS is illustrated in Fig. 1 (a).

**Variational Beam Search** A greedy search is prone to missing change points in data sets with a low signal/noise ratio per time step because it cannot accumulate evidence for a change point over a series of time steps. On the other end of the spectrum, the most expressive algorithm would involve assessing all possible sequences of  $\mathbf{s}_{\leq t} \in \{0, 1\}^t$  to determine the most likely set of shifts, and thus the most appropriate  $q_t(\mathbf{z}_t)$ ; however, this is not feasible due to scaling in  $O(2^t)$  for both compute and memory. The most obvious improvement over greedy search that has the ability to accumulate evidence for a change point is beam search. Rather than deciding greedily whether a change occurred or not at each time step, *variational beam search* (VBS) considers both cases in parallel, and it delays the decision of which one is more likely (see Fig. 1 (b) and Fig. 2 for illustration). The algorithm keeps track of a fixed number  $K > 1$  of possible sequences of change points. For each sequence, it iteratively updates a Gaussian variational distribution as in VGS. At time step  $t$ , every potential continuation of the  $K$  sequences is considered, with  $s_t \in \{0, 1\}$ , thus doubling the number of histories of which the algorithm has to keep track. To keep the computational requirements bounded, beam search thus discards half of the sequences based on an exploration-exploitation trade-off.

As follows, we describe how VBS proceeds from time  $t - 1$  to time  $t$ . At time  $t - 1$ , VBS will have a fixed set  $\mathbb{B}_{t-1}$  of  $K$  different ‘‘histories’’, i.e., a set of possible realizations of the change variable  $\mathbf{s}_{\leq t-1} \equiv \{s_0, \dots, s_{t-1}\}$  to which the

model has assigned high probabilities in previous iterations. These probabilities are given by the approximate posteriors over the change variables  $q(\mathbf{s}_{\leq t-1})$ , defined below. We stress that this is no longer a simple factorized distribution.

Similar to VGS, for each history  $\mathbf{s}_{\leq t-1} \in \mathbb{B}_{t-1}$ , we obtain  $q(\mathbf{z}_t|s_t = 0, \mathbf{s}_{\leq t-1})$  and  $q(\mathbf{z}_t|s_t = 1, \mathbf{s}_{\leq t-1})$  by optimizing the conditional ELBO (Eq.4), along with the respective binary mixture weights  $q(s_t = 0|\mathbf{s}_{\leq t-1}) \equiv m$  and  $q(s_t = 1|\mathbf{s}_{\leq t-1}) \equiv 1 - m$ . This results in  $2K$  possible sequences to choose from. This is pared down to  $K$  histories again by choosing the sequences resulting in the highest values of the un-normalized distributions  $q^*(\mathbf{s}_{\leq t}) := q(\mathbf{s}_{\leq t-1})q(s_t|\mathbf{s}_{\leq t-1})$  which we then normalize as  $q(\mathbf{s}_{\leq t}) = \frac{q^*(\mathbf{s}_{\leq t})}{\sum_{\mathbf{s}_{\leq t} \in \mathbb{B}_t} q^*(\mathbf{s}_{\leq t})}$ . Those remaining  $K$  sequences form  $\mathbb{B}_t$ . This concludes the recursion. This search strategy scales linearly in both compute and memory to  $K$ .

**Beam Search Diversification** Empirically, we find that the naive beam search procedure does not reveal its full potential. As commonly encountered in beam search, histories over change points are largely shared among all members of the beam. To encourage diverse beams, we constructed the following simple scheme: Let  $K$  be the number of hypotheses in a beam. While transitioning from time  $t - 1$  to  $t$ , every hypothesis splits into two scenarios, one with  $s_t = 0$  and one with  $s_t = 1$ , resulting in  $2K$  hypotheses. If two resulting hypotheses only differ in their most recent  $s_t$ -value, we say that they come from the same ‘‘family.’’ Each member among the  $2K$  hypotheses is ranked according to its ELBO value (Eq. 4). In a first step, we discard the bottom  $1/3$  of the  $2K$  hypotheses, leaving  $4/3K$  hypotheses (we always take integer multiples of 3 for  $K$ ). To truncate the beam size from  $4/3K$  down to  $K$ , we rank the remaining hypotheses according to their ELBO and pick the top  $K$  ones while *also* ensuring that we pick a member from every remaining family. The diversification scheme ensures that underperforming families can survive, leading to a more diverse set of hypotheses. We found this beam diversification scheme to work robustly across a variety of experiments.

## 4. Experiments

**Overview** The objective of our experiments is to show that compared to other methods, variational beam search (1) better reacts to distribution shifts in supervised setups, while (2) revealing interpretable and temporally sparse latent structure in unsupervised setups. To this end, we experiment on artificial data (Section 4.1), evaluate online linear regression on three datasets with distribution shifts (Section 4.3), study Bayesian deep learning approaches on sequences of transformed images (4.4), and study the dynamics of word embeddings on historical text corpora (Section 4.5). Unstated experimental details are in Supplement F.

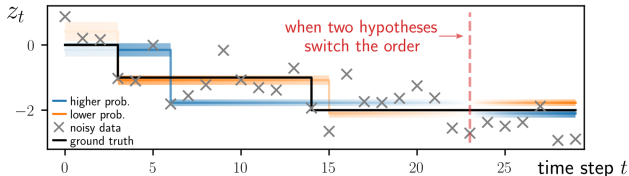


Figure 2. Inferring the mean (black line) of a time-varying data distribution (black samples) with VBS. The initially unlikely hypothesis begins dominating over the other at step 23.

#### 4.1. An Illustrative Example

We first aim to provide a basic intuition on VBS based on a simple setup involving artificial data. To this end, we simulated noisy data points centered around a piecewise-constant step function involving two steps (seen as in black in Fig. 2). We then used VBS with beam size 2 to fit the same model that generated the data. The ranking among both hypotheses at each moment in time is indicated by their color (blue as "more likely" vs. orange as "less likely"). While hypothesis 1 assumes a single distribution shift (initially blue), the hypothesis 2 (initially orange) assumes two shifts. We see that hypothesis 1 is initially more likely, but gets over-ruled by hypothesis 2 at later times (note the color swap at step 23). This shows that VBS can track multiple hypotheses over change points and do adjustments over time.

#### 4.2. Baselines

In our supervised experiments (Section 4.3 and Section 4.4), we compared VBS against established Bayesian online learning baselines and an independent batch learning baseline. In addition to Variational Continual Learning (VCL, see Section 3.1), we also compared against Laplace Propagation (LP) (Smola et al., 2003) (see also (Nguyen et al., 2018) for LP). Finally, we also adopt a trivial baseline: learning independent regressors/classifiers on each task. Here, we adopt both a Bayesian and a non-Bayesian approach. For VBS, we always report the dominant hypothesis.

In the unsupervised experiments (Section 4.5), we compared against the online version of dynamic word embeddings with a diffusion prior (Bamler & Mandt, 2017), which is a version of VCL. As described in this section, the focus is here on interpretability and temporal sparsity.

#### 4.3. Bayesian Linear Regression Experiments

As a simple first version of VBS, we tested an online linear regression setup for which the posterior can be computed analytically. The analytical solution removes the approximation error of the variational inference procedure as well as optimization-related artifacts since closed-form updates are available. Detailed derivations are in Supplement D.

Table 1. Evaluation of Different Datasets

MODELS	CIFAR-10 (ACCURACY)↑	SVHN	MALWARE	SENSORDRIFT (MCAE $10^{-2}$ )↓	ELEC2
VBS (K=6)*	<b>69.2±0.9</b>	<b>89.6±0.5</b>	<b>11.6±0.9</b>	<b>14.3±3.8</b>	<b>7.3±0.7</b>
VBS (K=3)*	68.9±0.9	89.1±0.5	<b>11.6±0.8</b>	15.5±4.7	<b>7.3±0.7</b>
VGS*	68.2±0.8	88.9±0.5	11.7±0.9	15.5±4.7	<b>7.3±0.7</b>
VCL <sup>†</sup>	66.7±0.8	88.7±0.5	13.3±0.8	24.9±12.9	16.6±1.0
LP <sup>‡</sup>	62.6±1.0	82.8±0.9	13.3±0.8	24.9±12.9	16.6±1.0
IT <sup>§</sup>	63.7±0.5	85.5±0.7	16.6±0.5	27.7±12.2	12.5±0.8
IT <sup>§</sup> (BAYES)	64.5±0.3	87.8±0.1	16.6±0.5	27.7±12.2	12.5±0.8

\* PROPOSED, <sup>†</sup> [NGUYEN ET AL., 2018], <sup>‡</sup> [SMOLA ET AL., 2003]

<sup>§</sup> INDEPENDENT TASK

We investigated three real-world datasets with natural temporal distribution shifts:

- **Malware** This data set is a collection of 100K malicious and benign computer programs, collected over 44 months (Huynh et al., 2017). Each program has 482 counting features and a real-valued probability  $p \in [0, 1]$  of being malware. We linearly predicted the log-odds.
- **SensorDrift** A collection of chemical sensor readings (Vergara et al., 2012). We focused on the gas *acetaldehyde*, whose 2926 samples span 36 months. We predicted the gas concentration level given 128 other features.
- **Elec2** The dataset contains the electricity price over three years of two Australian states (Harries & Wales, 1999). While the original problem was 0-1 binary classification, we reproduced the targets with real-valued probabilities. After processing, we had 45263 samples, and each sample comprised 14 features.

We split every dataset into a train, validation, and test set. We evaluated all methods with one-step ahead absolute error<sup>3</sup> and computed the mean cumulative absolute error (MCAE) for each observation. In Table 1, we reported the mean and the standard deviation of all MCAEs. VBS significantly outperforms all baselines. Please see data split details and more temporal results in Supplement F.2.

#### 4.4. Bayesian Deep Learning Experiments

Our larger-scale experiments involve Bayesian neural networks, trained on sequential classification tasks. We considered batches of CIFAR-10 and SVHN images. Every few tasks we transform all images globally by combining rotations, shifts, and scaling transformations.

**Datasets** We used two standard datasets for image classification: CIFAR-10 (Krizhevsky et al., 2009) and SVHN

<sup>3</sup>We measure the error in the probability space for classification problems (Malware and Elec2) and the error in the data space for regression problems (SensorDrift).

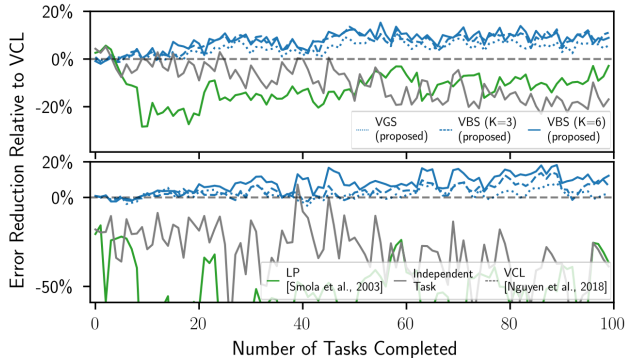


Figure 3. Test performance of our proposed VBS and VGS algorithms compared to various baselines (see main text) on transformed CIFAR-10 (top) and SVHN (bottom).

(Netzer et al., 2011). We adopted the original training set and used the first 5000 images in the original test set as the validation set and the others as the test set. We further split the training set into batches (or tasks in the continual learning literature) for online learning, each batch consisting of a third of the full data. Each transformation (either rotation, translation, or scaling) is generated from a fixed, predefined distribution (see Supplement F.3). Changes are introduced every three tasks, where the total number of tasks was 100.

**Architectures and Protocol** All Bayesian and non-Bayesian methods use the same neural network architecture. We used a truncated version of the VGG convolutional neural network on both datasets. We confirmed that our architecture achieved similar performance on CIFAR10 compared to the results reported by Zenke et al. (2017) and Lopez-Paz & Ranzato (2017) in a similar setting. We initialize each algorithm by training the model on the full, untransformed dataset. We set the tempering constant  $\beta = 2/3$  and let the conditional ELBO temperature  $T = 20000$  (in Eq. 7) for all supervised experiments. During every new task, all algorithms are trained until convergence. Please see details on network architectures and optimization algorithms in Supplement F.3.

**Results** Fig. 3 shows our main results on CIFAR-10 (top) and SVHN (bottom). To account for varying task difficulties, we show the percentage of the error reduction relative to our main baseline, VCL.

VBS with a large beam size of  $K = 6$  performs best, followed by VBS with  $K = 3$ . Variational greedy search (VGS), which corresponds to a beam size  $K = 1$ , performed better than VCL but worse than VBS. Table 1 shows the absolute performances of all considered methods, averaged across all of the 100 tasks for the two datasets. Our proposed methods improve over the best-performing baseline VCL by 0.9 percentage points on SVHN and 2.5 percentage points

on CIFAR-10. The effect of beam search is also evident, with larger beam sizes consistently performing better.

#### 4.5. Unsupervised Experiments

Our third experiment focused on unsupervised learning. Our focus was different: instead of showing performance improvements in terms of higher accuracy, we demonstrated that VBS helps uncover interpretable latent structure in high-dimensional time series, such as localizing changes in the individual words’ meanings over long periods. We also showed that these word embedding trajectories are useful for document dating.

**Datasets** We analyzed three large time-stamped text corpora, all of which are available online. Our first dataset is the Google Books corpus (Michel et al., 2011) consisting of  $n$ -grams, which is sufficient for learning word embeddings. We focused on the period from 1900 to 2000. To have an approximately even amount of data per year, we sub-sampled 250M to 300M tokens per year. Second, we used the Congressional Records data set (Gentzkow et al., 2018), which has 13M to 52M tokens per two-year period from 1875 to 2011. Third, we used the UN General Debates corpus (Jankin Mikhaylov et al., 2017), which has about 250k to 450k tokens per year from 1970 to 2018. For all three corpora, the vocabulary size used was 30000 for qualitative results and 10000 for quantitative results. We further randomly split the corpus of every time step into training set (90%) and heldout test set (10%).

**Model** To analyze the semantic changes of individual words over time, we used Dynamic Word Embeddings (Bamler & Mandt, 2017) as our base model in all experiments. The model relies on a probabilistic interpretation of Word2Vec and learns smooth word embedding trajectories by imposing a time-series prior on the embeddings. For our proposed approach, we imposed our spike and slab novelty prior (Eq. 3) that induces temporal sparsity, allowing us to time-localize semantic changes of words. We set the tempering constant  $\beta = 0.5$  for Google books and Congressional records and let  $\beta = 0.25$  for UN debates. We combined this prior with beam search ( $K = 8$ ) and we reported all eight hypotheses’ results. In contrast to the supervised learning experiments, we set  $T = 1$  in Eq. 7.

We also considered regular word embeddings trained on individual years (Mikolov et al., 2013). While (Bamler & Mandt, 2017) already carried-out the comparison to dynamic word embeddings, we used them to measure the compressibility of word embeddings for document dating tasks, as we describe below.

**Qualitative Results** Our first experiments demonstrate that a spike and slab prior is more interpretable and results

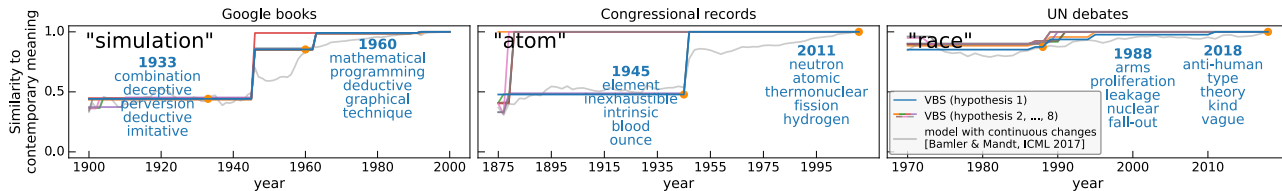


Figure 4. Dynamic Word Embeddings on Google books, Congressional records, and UN debates, trained with VBS (proposed, colorful) vs. VCL (grey). In contrast to VCL, VBS reveals sparse, time-localized semantic changes (see main text).

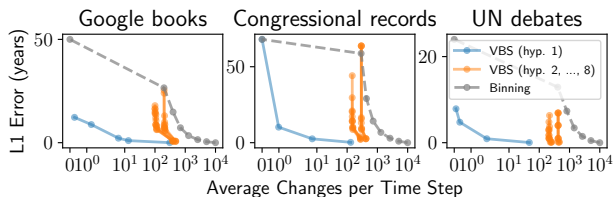


Figure 5. Document dating error as a function of model sparsity, measured in average words updates per year. As semantic changes get successively sparsified by varying  $\xi_0$  (Eq. 7), VBS maintains a better document dating performance compared to baselines.

in more meaningful word semantics than the diffusion prior of (Bamler & Mandt, 2017). Figure 4 shows three selected words (“simulation”, “atom”, and “race”—one taken from each corpus) and their nearest neighbors in latent space. As time progresses the nearest neighboring words change, reflecting a semantic change of the words. While the horizontal axis shows the year, the vertical axis shows the cosine distance of the word’s embedding vector at the given year to its embedding vector in the last available year.

The plot reveals several interpretable semantic changes of each word captured by VBS. For example, as shown by the most likely hypothesis in blue for the Congressional Records data, the term “atom” changes its meaning from “element” to “nuclear” in 1945—the year when two nuclear bombs were detonated. The word “race” changes from the cold-war era “arms”(-race) to its more prevalent meaning after 1991 when the cold war ended. The word “simulation” changes its dominant context from “deception” to “programming” with the advent of computers. The plot also showcases various possible semantic changes of all eight hypotheses, where each hypothesis states various aspects.

**Quantitative Results** Dynamic word embeddings can be useful for document dating, essentially by testing which year’s word vectors assign the highest probability to the observed word-context pairs of a given document (Bamler & Mandt, 2017). Dynamic word embeddings are stored as a list of embedding vectors with associated time stamps—one vector per update, and usually one update per year. This can result in large file sizes. For a quantitative evaluation

of VBS, we ask how much we can compress these representations by suppressing temporal changes. This naturally incurs a loss in document dating accuracy. The tradeoff between loss in dating performance (L1 error) and sparsity of changes (linearly affecting the file size) can be understood as a classical rate-distortion tradeoff in the compression sense.

Figure 5 shows the results on the three corpora data, where we plot the document dating error as a function of allowed changes per year, with 10000 changes (vocabulary size) at maximum. For fewer allowed semantic changes per year, the dating error goes up. Lower curves are better. As a simple baseline, we assumed that we had separate word embeddings associated with episodes of  $L$  consecutive years. For  $T$  years in total, the associated memory requirements would be proportional to  $V * T / L$ , where  $V$  is the vocabulary size. Assuming we could perfectly date the document up to  $L$  years results in the “binning” baseline in Figure 5. For VBS, we show the dominant hypothesis (blue) as well as the subleading hypotheses (orange). The most likely hypothesis of VBS clearly outperforms the baseline, leading to higher document dating precision at much smaller file size.

## 5. Conclusions

We introduced variational beam search: an approximate inference algorithm for continual learning on non-stationary data with irregular changes. Our approach mediates the tradeoff between catastrophic forgetting (i.e., losing the information obtained on previous tasks) and catastrophic remembering (i.e., becoming overconfident and unable to adapt to new data). It is based on a Bayesian treatment of a given model’s parameters and aimed at optimally tuning them towards the most recent learning task. To this end, we introduced a sequence of a discrete change variables whose value controlled the way we regularized the model. For no detected change, we regularized the new task towards the previously learned solution; for a detected change, we broadened the prior to give room for new data evidence. This procedure is combined with beam search over the discrete change variable. In different experiments, we showed that our proposed model (1) achieved lower error in supervised setups, and (2) revealed a more interpretable and compressible latent structure in unsupervised experiments.



## Acknowledgements

We gratefully acknowledge extensive contributions from Robert Bamler (previously UCI, now University of Tübingen), which were indispensable to this work.

This material is based upon work supported in part by the National Science Foundation under grant numbers 1633631, 1928718, 2003237, and 2007719; by the National Science Foundation Graduate Research Fellowship under grant number DGE-1839285; by the Center for Statistics and Applications in Forensic Evidence (CSAFE) through Cooperative Agreement 70NANB20H019 between NIST and Iowa State University, which includes activities carried out at University of California Irvine; by the Defense Advanced Research Projects Agency (DARPA) under Contract No. HR001120C0021; by an Intel grant; and by grants from Qualcomm. Any opinion, findings, and conclusions or recommendations expressed in this material are those of the authors and do not necessarily reflect the views of the National Science Foundation, nor do they reflect the views of DARPA.

## References

- Adams, R. P. and MacKay, D. J. Bayesian online changepoint detection. *arXiv preprint arXiv:0710.3742*, 2007.
- Aljundi, R., Kelchtermans, K., and Tuytelaars, T. Task-free continual learning. In *Proceedings of the IEEE Conference on Computer Vision and Pattern Recognition*, pp. 11254–11263, 2019.
- Bamler, R. and Mandt, S. Dynamic word embeddings. In *Proceedings of the 34th International Conference on Machine Learning-Volume 70*, pp. 380–389. JMLR. org, 2017.
- Barber, D. *Bayesian reasoning and machine learning*. Cambridge University Press, 2012.
- Becker-Ehmck, P., Peters, J., and Van Der Smagt, P. Switching linear dynamics for variational bayes filtering. In *International Conference on Machine Learning*, pp. 553–562, 2019.
- Bishop, C. M. et al. *Neural networks for pattern recognition*. Oxford university press, 1995.
- Bracegirdle, C. and Barber, D. Switch-reset models: Exact and approximate inference. In *Proceedings of The Fourteenth International Conference on Artificial Intelligence and Statistics*, pp. 190–198, 2011.
- Buslaev, A., Igloukov, V. I., Khvedchenya, E., Parinov, A., Druzhinin, M., and Kalinin, A. A. Albumentations: Fast and flexible image augmentations. *Information*, 11(2), 2020. ISSN 2078-2489. doi: 10.3390/info11020125.
- URL <https://www.mdpi.com/2078-2489/11/2/125>.
- Farquhar, S. and Gal, Y. A unifying bayesian view of continual learning. *Third workshop on Bayesian Deep Learning (NeurIPS 2018)*, 2018.
- Fearnhead, P. Exact bayesian curve fitting and signal segmentation. *IEEE Transactions on Signal Processing*, 53(6):2160–2166, 2005.
- Fearnhead, P. and Liu, Z. On-line inference for multiple changepoint problems. *Journal of the Royal Statistical Society: Series B (Statistical Methodology)*, 69(4):589–605, 2007.
- Friedman, J., Hastie, T., and Tibshirani, R. *The elements of statistical learning*, volume 1. Springer series in statistics New York, 2001.
- Gentzkow, M., Shapiro, J., and Taddy, M. Congressional record for the 43rd-114th congresses: Parsed speeches and phrase counts. In URL: <https://data.stanford.edu/congress text>, 2018.
- Glorot, X. and Bengio, Y. Understanding the difficulty of training deep feedforward neural networks. In *Proceedings of the thirteenth international conference on artificial intelligence and statistics*, pp. 249–256, 2010.
- Goodfellow, I. J., Mirza, M., Da Xiao, A. C., and Bengio, Y. An empirical investigation of catastrophic forgetting in gradientbased neural networks. In *In Proceedings of International Conference on Learning Representations (ICLR. Citeseer*, 2014.
- Harries, M. and Wales, N. S. Splice-2 comparative evaluation: Electricity pricing. 1999.
- Hoffman, M. D. and Blei, D. M. Structured stochastic variational inference. In *Artificial Intelligence and Statistics*, 2015.
- Huynh, N. A., Ng, W. K., and Ariyapala, K. A new adaptive learning algorithm and its application to online malware detection. In *International Conference on Discovery Science*, pp. 18–32. Springer, 2017.
- Jankin Mikhaylov, S., Baturo, A., and Dasandi, N. United Nations General Debate Corpus, 2017. URL <https://doi.org/10.7910/DVN/0TJX8Y>.
- Jordan, M. I., Ghahramani, Z., Jaakkola, T. S., and Saul, L. K. An introduction to variational methods for graphical models. *Machine learning*, 37(2):183–233, 1999.
- Kalman, R. E. A new approach to linear filtering and prediction problems. *Journal of Basic Engineering*, pp. 82(1):35–45, 1960.

- Kingma, D. P. and Ba, J. Adam: A method for stochastic optimization. *arXiv preprint arXiv:1412.6980*, 2014.
- Kingma, D. P. and Welling, M. Auto-encoding variational bayes. *arXiv preprint arXiv:1312.6114*, 2013.
- Kirkpatrick, J., Pascanu, R., Rabinowitz, N., Veness, J., Desjardins, G., Rusu, A. A., Milan, K., Quan, J., Ramalho, T., Grabska-Barwinska, A., et al. Overcoming catastrophic forgetting in neural networks. *Proceedings of the national academy of sciences*, 114(13):3521–3526, 2017.
- Krizhevsky, A., Hinton, G., et al. Learning multiple layers of features from tiny images. 2009.
- Kurle, R., Cseke, B., Klushyn, A., van der Smagt, P., and Günnemann, S. Continual learning with bayesian neural networks for non-stationary data. In *International Conference on Learning Representations*, 2020.
- Lee, S., Ha, J., Zhang, D., and Kim, G. A neural dirichlet process mixture model for task-free continual learning. In *International Conference on Learning Representations*, 2020.
- Linderman, S., Johnson, M., Miller, A., Adams, R., Blei, D., and Paninski, L. Bayesian learning and inference in recurrent switching linear dynamical systems. In *Artificial Intelligence and Statistics*, pp. 914–922, 2017.
- Lopez-Paz, D. and Ranzato, M. Gradient episodic memory for continual learning. In *Advances in neural information processing systems*, pp. 6467–6476, 2017.
- Michel, J.-B., Shen, Y. K., Aiden, A. P., Veres, A., Gray, M. K., Pickett, J. P., Hoiberg, D., Clancy, D., Norvig, P., Orwant, J., et al. Quantitative analysis of culture using millions of digitized books. *science*, 331(6014):176–182, 2011.
- Mikolov, T., Sutskever, I., Chen, K., Corrado, G. S., and Dean, J. Distributed representations of words and phrases and their compositionality. In *Advances in neural information processing systems*, pp. 3111–3119, 2013.
- Murphy, K. P. *Machine learning: a probabilistic perspective*. MIT press, 2012.
- Netzer, Y., Wang, T., Coates, A., Bissacco, A., Wu, B., and Ng, A. Y. Reading digits in natural images with unsupervised feature learning. 2011.
- Nguyen, C. V., Li, Y., Bui, T. D., and Turner, R. E. Variational continual learning. In *International Conference on Learning Representations*, 2018.
- Ovadia, Y., Fertig, E., Ren, J., Nado, Z., Sculley, D., Nowozin, S., Dillon, J. V., Lakshminarayanan, B., and Snoek, J. Can you trust your model’s uncertainty? evaluating predictive uncertainty under dataset shift. In *Advances in Neural Information Processing Systems*, 2019.
- Ranganath, R., Gerrish, S., and Blei, D. Black box variational inference. In *Artificial Intelligence and Statistics*, pp. 814–822, 2014.
- Rao, D., Visin, F., Rusu, A., Pascanu, R., Teh, Y. W., and Hadsell, R. Continual unsupervised representation learning. In *Advances in Neural Information Processing Systems*, pp. 7647–7657, 2019.
- Rusmassen, C. and Williams, C. Gaussian process for machine learning, 2005.
- Schwarz, J., Altman, D., Dudzik, A., Vinyals, O., Teh, Y. W., and Pascanu, R. Towards a natural benchmark for continual learning. In *NeurIPS Workshop on Continual Learning*, 2018.
- Shin, H., Lee, J. K., Kim, J., and Kim, J. Continual learning with deep generative replay. In *Advances in Neural Information Processing Systems*, pp. 2990–2999, 2017.
- Smola, A. J., Vishwanathan, V., and Eskin, E. Laplace propagation. In *NIPS*, pp. 441–448, 2003.
- Titsias, M. K., Schwarz, J., Matthews, A. G. d. G., Pascanu, R., and Teh, Y. W. Functional regularisation for continual learning with gaussian processes. In *International Conference on Learning Representations*, 2019.
- Titsias, M. K., Sygnowski, J., and Chen, Y. Sequential changepoint detection in neural networks with checkpoints. *arXiv preprint arXiv:2010.03053*, 2020.
- Vergara, A., Vembu, S., Ayhan, T., Ryan, M. A., Homer, M. L., and Huerta, R. Chemical gas sensor drift compensation using classifier ensembles. *Sensors and Actuators B: Chemical*, 166:320–329, 2012.
- Wainwright, M. J. and Jordan, M. I. Graphical models, exponential families, and variational inference. *Foundations and Trends® in Machine Learning*, 1(1-2):1–305, 2008.
- Wen, Y., Vicol, P., Ba, J., Tran, D., and Grosse, R. Flipout: Efficient pseudo-independent weight perturbations on mini-batches. In *International Conference on Learning Representations*, 2018.
- Xie, Y., Huang, J., and Willett, R. Change-point detection for high-dimensional time series with missing data. *IEEE Journal of Selected Topics in Signal Processing*, 7(1): 12–27, 2012.
- Xuan, X. and Murphy, K. Modeling changing dependency structure in multivariate time series. In *Proceedings of the 24th international conference on Machine learning*, pp. 1055–1062, 2007.

- Zech, J. R., Badgeley, M. A., Liu, M., Costa, A. B., Titano, J. J., and Oermann, E. K. Variable generalization performance of a deep learning model to detect pneumonia in chest radiographs: a cross-sectional study. *PLoS medicine*, 15(11):e1002683, 2018.
- Zenke, F., Poole, B., and Ganguli, S. Continual learning through synaptic intelligence. *Proceedings of machine learning research*, 70:3987, 2017.
- Zhang, C., Bütepage, J., Kjellström, H., and Mandt, S. Advances in variational inference. *IEEE transactions on pattern analysis and machine intelligence*, 41(8):2008–2026, 2018.

---

# Variational Beam Search for Learning with Distribution Shifts: Supplementary Materials

---

## A. Structured Variational Inference

According to the main paper, we consider the generative model  $p_\beta(\mathbf{x}_t, \mathbf{z}_t, s_t) = p(s_t)p_\beta(\mathbf{z}_t|s_t)p(\mathbf{x}_t|\mathbf{z}_t)$  at time step  $t$ . Upon observing the data  $\mathbf{x}_t$ , both  $\mathbf{z}_t$  and  $s_t$  are inferred. However, exact inference is not available due to the intractability of the marginal likelihood (Eq. 5 in the main paper). To tackle this, we utilize structured variational inference for both the latent variables  $\mathbf{z}_t$  and the Bernoulli change variable  $s_t$ . To this end, we define the joint variational distribution  $q(\mathbf{z}_t, s_t) = q(s_t)q(\mathbf{z}_t|s_t)$ . Then the updating procedure for  $q(s_t)$  and  $q(\mathbf{z}_t|s_t)$  is obtained by maximizing the ELBO  $\mathcal{L}(q)$ :

$$q_t(\mathbf{z}_t, s_t) = \arg \max_{q(\mathbf{z}_t, s_t) \in \mathcal{Q}} \mathcal{L}(q),$$

$$\mathcal{L}(q) := \mathbb{E}_q[\log p_\beta(\mathbf{x}_t, \mathbf{z}_t, s_t) - \log q(\mathbf{z}_t, s_t)].$$

Given the generative models, we can further expand  $\mathcal{L}(q)$  to simplify the optimization:

$$\begin{aligned} \mathcal{L}(q) &= \mathbb{E}_{q(s_t)q(\mathbf{z}_t|s_t)}[\log p(s_t) + \log p_\beta(\mathbf{z}_t|s_t) + \log p(\mathbf{x}_t|\mathbf{z}_t) - \log q(s_t) - \log q(\mathbf{z}_t|s_t)] \\ &= \mathbb{E}_{q(s_t)}[\log p(s_t) - \log q(s_t) + \mathbb{E}_{q(\mathbf{z}_t|s_t)}[\log p_\beta(\mathbf{z}_t|s_t) + \log p(\mathbf{x}_t|\mathbf{z}_t) - \log q(\mathbf{z}_t|s_t)]] \\ &= \mathbb{E}_{q(s_t)}[\log p(s_t) - \log q(s_t) + \mathbb{E}_{q(\mathbf{z}_t|s_t)}[\log p(\mathbf{x}_t|\mathbf{z}_t)] - \text{KL}(q(\mathbf{z}_t|s_t)||p_\beta(\mathbf{z}_t|s_t))] \\ &= \mathbb{E}_{q(s_t)}[\log p(s_t) - \log q(s_t) + \mathcal{L}(q|s_t)] \end{aligned} \quad (9)$$

where the second step pushes inside the expectation with respect to  $q(\mathbf{z}_t|s_t)$ , the third step re-orders the terms, and the final step utilizes the definition of conditional ELBO (Eq. 4 in the main paper).

Maximizing Eq. 9 therefore implies a two-step optimization: first maximize the conditional ELBO  $\mathcal{L}(q|s_t)$  to find the optimal  $q_t(\mathbf{z}_t|s_t = 1)$  and  $q_t(\mathbf{z}_t|s_t = 0)$ , then compute the Bernoulli distribution  $q^*(s_t)$  by maximizing  $\mathcal{L}(q)$  while the conditional ELBOs  $\mathcal{L}(q_t|s_t)$  are fixed.

While  $q_t(\mathbf{z}_t|s_t)$  typically needs to be inferred by black box variational inference (Ranganath et al., 2014; Kingma & Welling, 2013; Zhang et al., 2018), the optimal  $q^*(s_t)$  has a closed-form solution and bears resemblance to the exact inference counterpart (Eq. 6 in the main paper). To see this, we assume  $\mathcal{L}(q_t|s_t)$  are given and  $q(s_t)$  is parameterized by  $m \in \mathbb{R}$  (for the Bernoulli distribution). Rewriting Eq. 9 gives

$$\mathcal{L}(q) = m(\log p(s_t = 1) - \log m + \mathcal{L}(q_t|s_t = 1)) + (1 - m)(\log p(s_t = 0) - \log(1 - m) + \mathcal{L}(q_t|s_t = 0))$$

which is concave since the second derivative is negative. Thus taking the derivative and setting it to zero leads to the optimal solution of

$$\begin{aligned} \log \frac{m}{1 - m} &= \log p(s_t = 1) - \log p(s_t = 0) + \mathcal{L}(q_t|s_t = 1) - \mathcal{L}(q_t|s_t = 0), \\ m &= \sigma(\mathcal{L}(q_t|s_t = 1) - \mathcal{L}(q_t|s_t = 0)) + \xi_0, \end{aligned}$$

which attains the closed-form solution as stated in Eq. 7 in the main paper without temperature  $T$ .

## B. Additive vs. Multiplicative Broadening

There are several possible choices for defining a posterior broadening functional. In latent time series models, such as latent Kalman filters (Kalman, 1960; Bamler & Mandt, 2017), it is common to convolve the previous posterior with a Gaussian transition kernel  $K(\cdot)$ , resulting in  $\mathcal{F}(q_{t-1})(\mathbf{z}_t) = \int K(\mathbf{z}_t - \mathbf{z}'_t)q_{t-1}(\mathbf{z}'_t)d\mathbf{z}'_t$ . Trivially,  $K(\mathbf{z}_t - \mathbf{z}'_t) = \delta(\mathbf{z}_t - \mathbf{z}'_t)$  results in Eq. 1 in the main paper as a special case. In detail, convolving the previous posterior with a Gaussian transition kernel

## Variational Beam Search for Learning with Distribution Shifts

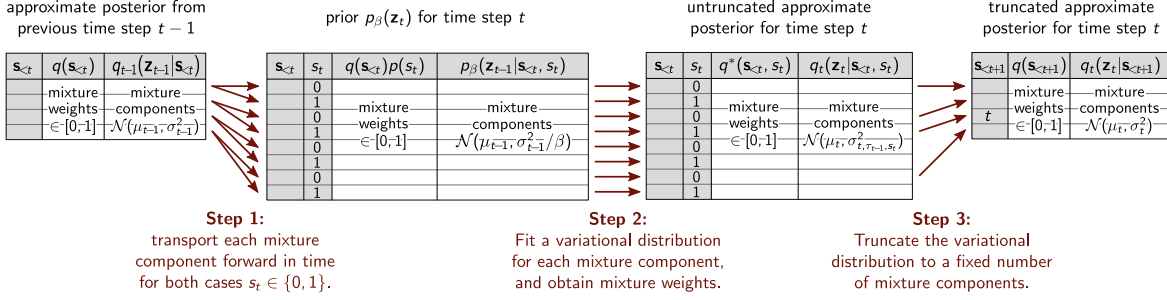


Figure 6. Conditional probability table of variational beam search

### Algorithm 1 Variational Beam Search

**Input:** task set  $\{\mathbf{x}_t\}_1^T$ ; beam size  $K$ ; prior log-odds  $\xi_0$ ; conditional ELBO temperature  $T$

**Output:** approximate posterior distributions  $\{q(\mathbf{s}_{0:t}), q_t(\mathbf{z}_t|\mathbf{s}_{0:t})\}_1^T$

- 1:  $q(s_0 = 0) := 1$ ;  $q_0(\mathbf{z}_0|s_0) := \mathcal{N}(\mathbf{z}_0; \mathbf{0}, \mathbf{1})$ ;  $\mathbb{B} = \{s_0 = 0\}$ ;
- 2: **for**  $t = 1, \dots, T$  **do**
- 3:  $\mathbb{B}' = \{\}$
- 4: **for** each hypothesis  $\mathbf{s}_{<t} \in \mathbb{B}$  **do**
- 5:  $p(s_t = 1) := \sigma(\xi_0)$  for random variable  $s_t \in \{0, 1\}$
- 6:  $\mathbb{B}' := \mathbb{B}' \cup \{(\mathbf{s}_{<t}, s_t = 0), (\mathbf{s}_{<t}, s_t = 1)\}$ ;
- 7: compute the task  $t$ 's prior  $p_\beta(\mathbf{z}_t|\mathbf{s}_{<t}, s_t)$  (Eq. 3);
- 8: perform structured variational inference (Eq. 4 and Eq. 7) given observation  $\mathbf{x}_t$ , resulting in  $q^*(s_t, \mathbf{z}_t) = q^*(s_t)q_t(\mathbf{z}_t|s_t)$  where  $q_t(\mathbf{z}_t|s_t)$  is stored as output  $q_t(\mathbf{z}_t|\mathbf{s}_{0:t})$ ;
- 9: approximate new hypotheses' posterior probability  $p(\mathbf{s}_{0:t}|\mathbf{x}_{1:t}) \approx q^*(\mathbf{s}_{<t}, s_t) = q(\mathbf{s}_{<t})q^*(s_t)$ ;
- 10: **end for**
- 11:  $\mathbb{B} := \text{diverse\_truncation}(\mathbb{B}', q^*(\mathbf{s}_{<t}, s_t))$ ;
- 12: normalize  $q^*(\mathbf{s}_{<t}, s_t)$  where  $(\mathbf{s}_{<t}, s_t) \in \mathbb{B}$ , resulting in  $q(\mathbf{s}_{0:t})$  for output and the next task;
- 13: **end for**

results in adding the variance of all variables with a constant determined by the kernel. We thus call this convolution scheme *additive broadening*. The problem with such a choice, however, is that the associated information loss is not homogeneously distributed: dimensions of  $\mathbf{z}_t$  with low posterior uncertainty lose more information relative to dimensions of  $\mathbf{z}_t$  that are already uncertain. We found that this scheme deteriorates the learning signal.

We therefore consider *multiplicative broadening* (or *relative broadening* since the associated information loss depends on the original variance) as *tempering* described in the main paper, resulting in  $\mathcal{F}_\beta(q_{t-1})(\mathbf{z}_t) \propto q_{t-1}(\mathbf{z}_t)^\beta$  for  $0 < \beta \leq 1$ . For a Gaussian distribution, the resulting variance scales the original variance with  $\frac{1}{\beta}$ . In practice, we found relative or multiplicative broadening to perform much better and robustly than additive posterior broadening by a convolution. Since tempering broadens the posterior non-locally, this scheme does not possess a continuous latent time series interpretation<sup>4</sup>.

## C. Details on “Shy” Variational Greedy Search and Variational Beam Search

**“Shy” Variational Greedy Search.** As illustrated in Fig. 1 in the main text, one obtains better interpretation if one outputs the variational parameters  $\mu_t$  and  $\sigma_t$  at the end of a segment of constant  $\mathbf{z}_t$ . More precisely, when the algorithm detects a change point  $s_t = 1$ , it outputs the variational parameters  $\mu_{t-1}$  and  $\sigma_{t-1}$  from just before the detected change point  $t$ . These parameters define a variational distribution that has been fitted, in an iterative way, to all data points since the preceding detected change point. We call this the “shy” variant of the variational greedy search algorithm, because this variant quietly iterates over the data and only outputs a new fit when it is as certain about it as it will ever be. The red lines and regions in Fig. 1 (a) in the main paper illustrate means and standard deviations outputted by the “shy” variant of variational greedy search.

<sup>4</sup>This means that it is impossible to specify a conditional distribution  $p(\mathbf{z}_t|\mathbf{z}_{t-1})$  that corresponds to relative broadening.

We applied this ‘‘Shy’’ variant to our illustrative example (Section 4.1) and unsupervised learning experiments (Section 4.5).

**Variational Beam Search.** As follows, we present a more detailed explanation of the variational beam search procedure outlined in Section 3.3 of the main paper. Our beam search procedure defines an effective way to search for potential hypotheses with regards to sequences of inferred change points. The procedure is completely defined by detailing three sequential steps, that when executed, take a set of hypotheses found at time step  $t - 1$  and transform them into the resulting set of likely hypotheses for time step  $t$  that have appropriately accounted for the new data seen at  $t$ . The red arrows in Figure 6 illustrate these three steps for beam search with a beam size of  $K = 4$ .

In Figure 6, each of the three steps maps a table of considered histories to a new table. Each table defines a mixture of Gaussian distributions where each mixture component corresponds to a different history and is represented by different a row in the table. We start on the left with the (truncated) variational distribution  $q_{t-1}(\mathbf{z}_{t-1})$  from the previous time step, which is a mixture over  $K = 4$  Gaussian distributions. Each mixture component (row in the table) is labeled by a 0-1 vector  $\mathbf{s}_{<t} = (s_0, s_1, \dots, s_{t-1})$  of the change variable values according to that history. Each mixture component  $\mathbf{s}_{<t}$  further has a mixture weight  $q(\mathbf{s}_{<t}) \in [0, 1]$ , a mean, and a standard deviation.

We then obtain a prior for time step  $t$  by transporting each mixture component of  $q_{t-1}(\mathbf{z}_{t-1})$  forward in time via the broadening functional (‘‘Step 1’’ in the above figure). The prior  $p_\beta(\mathbf{z}_t)$  (second table in the figure) is a mixture of  $2K$  Gaussian distributions because each previous history splits into two new ones for the two potential cases  $s_t \in \{0, 1\}$ . The label for each mixture component (table row) is a new vector  $(\mathbf{s}_{<t}, s_t)$  or  $\mathbf{s}_{<t+1}$ , appending  $s_t$  to the tail of  $\mathbf{s}_{<t}$ .

‘‘Step 2’’ in the above figure takes the data  $\mathbf{x}_t$  and fits a variational distribution  $q_t(\mathbf{z}_t)$  that is also a mixture of  $2K$  Gaussian distributions. To learn the variational distribution, we (i) numerically fit each mixture component  $q(\mathbf{z}_t | \mathbf{s}_{<t}, s_t)$  individually, using the corresponding mixture component of  $p_\beta(\mathbf{z}_t)$  as the prior; (ii) evaluate (or estimate) the conditional ELBO of each fitted mixture component, conditioned on  $(\mathbf{s}_{<t}, s_t)$ ; (iii) compute the approximate posterior probability  $q^*(s_t)$  of each mixture component, in the presence of the conditional ELBOs; and (iv) obtain the mixture weight equal to the posterior probability over  $(\mathbf{s}_{<t}, s_t)$ , i.e.,  $p(\mathbf{s}_{0:t} | \mathbf{x}_{1:t})$ , best approximated by  $q(\mathbf{s}_{<t})q^*(s_t)$ .

‘‘Step 3’’ in the above figure truncates the variational distribution by discarding  $K$  of the  $2K$  mixture components. The truncation scheme can be either the ‘‘vanilla’’ beam search or diversified beam search outlined in the main paper. The truncated variational distribution  $q_t(\mathbf{z}_t)$  is again a mixture of only  $K$  Gaussian distributions, and it can thus be used for subsequent update steps, i.e., from  $t$  to  $t + 1$ .

The pseudocode is listed in Algo 1.

## D. Online Bayesian Linear Regression with Variational Beam Search

This section will derive the analytical solution of online updates for both Bayesian linear regression and the probability of change variables. We consider Gaussian prior distributions for weights. The online update of the posterior distribution is straightforward in the natural parameter space, where the update is analytic given the sufficient statistics of the observations. If we further allow to temper the weights’ distributions with a fixed temperature  $\beta$ , then this corresponds to multiplying each element in the precision matrix by  $\beta$ . We applied this algorithm to the linear regression experiments in Section 4.3. For unified names, we still use the word ‘‘variational’’ even though the solutions are analytical.

### D.1. Variational Continual Learning for Online Linear Regression

Let’s start with assuming a generative model at time  $t$ :

$$\begin{aligned} \boldsymbol{\theta} &\sim \mathcal{N}(\boldsymbol{\mu}, \Sigma), \\ y_t &= \boldsymbol{\theta}^\top \mathbf{x}_t + \epsilon, \quad \epsilon \sim \mathcal{N}(0, \sigma_n^2), \end{aligned} \tag{10}$$

and the noise  $\epsilon$  is constant over time.

The posterior distribution of  $\boldsymbol{\theta}$  is of interest, which is Gaussian distributed since both the likelihood and prior are Gaussian. To get an online recursion for  $\boldsymbol{\theta}$ ’s posterior distribution over time, we consider the natural parameterization. The prior

distribution under this parameterization is

$$\begin{aligned} p(\boldsymbol{\theta}) &= \frac{1}{Z} \exp\left(-\frac{(\boldsymbol{\theta} - \boldsymbol{\mu})^\top \Sigma^{-1}(\boldsymbol{\theta} - \boldsymbol{\mu})}{2}\right) \\ &= \frac{1}{Z} \exp\left(-\frac{1}{2}\boldsymbol{\theta}^\top \Sigma^{-1}\boldsymbol{\theta} + \boldsymbol{\theta}^\top \Sigma^{-1}\boldsymbol{\mu}\right) \\ &= \frac{1}{Z} \exp\left(-\frac{1}{2}\boldsymbol{\theta}^\top \Lambda \boldsymbol{\theta} + \boldsymbol{\theta}^\top \boldsymbol{\eta}\right) \end{aligned}$$

where  $\Lambda = \Sigma^{-1}$ ,  $\boldsymbol{\eta} = \Sigma^{-1}\boldsymbol{\mu}$  are the natural parameters and the terms unrelated to  $\boldsymbol{\theta}$  are absorbed into the normalizer  $Z$ .

Following the same parameterization, the posterior distribution can be written

$$\begin{aligned} p(\boldsymbol{\theta}|\mathbf{x}_t, y_t) &\propto p(\boldsymbol{\theta})p(y_t|\mathbf{x}_t, \boldsymbol{\theta}) \\ &= \frac{1}{Z} \exp\left(-\frac{1}{2}\boldsymbol{\theta}^\top \Lambda \boldsymbol{\theta} + \boldsymbol{\theta}^\top \boldsymbol{\eta} - \frac{1}{2}\sigma_n^{-2}\boldsymbol{\theta}^\top (\mathbf{x}_t \mathbf{x}_t^\top) \boldsymbol{\theta} + \sigma_n^{-2}y_t \boldsymbol{\theta}^\top \mathbf{x}_t\right) \\ &= \frac{1}{Z} \exp\left(-\frac{1}{2}\boldsymbol{\theta}^\top (\Lambda + \sigma_n^{-2}\mathbf{x}_t \mathbf{x}_t^\top) \boldsymbol{\theta} + \boldsymbol{\theta}^\top (\boldsymbol{\eta} + \sigma_n^{-2}y_t \mathbf{x}_t)\right). \end{aligned}$$

Thus we get the recursion over the natural parameters

$$\begin{aligned} \Lambda' &= \Lambda + \sigma_n^{-2}\mathbf{x}_t \mathbf{x}_t^\top, \\ \boldsymbol{\eta}' &= \boldsymbol{\eta} + \sigma_n^{-2}y_t \mathbf{x}_t, \end{aligned}$$

from which the posterior mean and covariance can be solved.

## D.2. Prediction and Marginal Likelihood

We can get the posterior predictive distribution for a new input  $\mathbf{x}_*$  through inspecting Eq. 10 and utilizing the linear properties of Gaussian. Assuming the generative model as specified above, we replace  $\mathbf{x}_t$  with  $\mathbf{x}_*$  in Eq. 10. Since  $\boldsymbol{\theta}$  is Gaussian distributed, by its linear property,  $\mathbf{x}_*^\top \boldsymbol{\theta}$  conforms to  $\mathcal{N}(\mathbf{x}_*^\top \boldsymbol{\mu}; \mathbf{x}_*^\top \boldsymbol{\mu}, \mathbf{x}_*^\top \Sigma \mathbf{x}_*)$ . Then the addition of two independent Gaussian results in  $y_* \sim \mathcal{N}(y_*; \mathbf{x}_*^\top \boldsymbol{\mu}, \sigma_n^2 + \mathbf{x}_*^\top \Sigma \mathbf{x}_*)$ .

The marginal likelihood shares this same form with the posterior predictive distribution, with a potentially different pair of sample  $(\mathbf{x}, y)$ . To see this, given a prior distribution  $\boldsymbol{\theta} \sim \mathcal{N}(\boldsymbol{\theta}; \boldsymbol{\mu}, \Sigma)$ , then the marginal likelihood of  $y|\mathbf{x}$  is

$$\begin{aligned} p(y|\mathbf{x}; \boldsymbol{\mu}, \Sigma, \sigma_n) &= \int p(y|\mathbf{x}, \boldsymbol{\theta})p(\boldsymbol{\theta}; \boldsymbol{\mu}, \Sigma)d\boldsymbol{\theta} \\ &= \mathcal{N}(y; \mathbf{x}^\top \boldsymbol{\mu}, \sigma_n^2 + \mathbf{x}^\top \Sigma \mathbf{x}) \end{aligned} \quad (11)$$

with  $\sigma_n^2$  being the noise variance. Note that in variational inference with an intractable marginal likelihood (not like the linear regression here), this is the approximated objective (Evidence Lower Bound (ELBO), indeed) we aim to maximize.

**Computation of the Covariance Matrix** Since we parameterize the precision matrix instead of the covariance matrix, the variance of the new test sample requires to take the inverse of the precision matrix. In order to do this, we employ the eigendecomposition of the precision matrix and re-assemble to the covariance matrix through inverting the eigenvalues.

**Logistic Normal Model** If we are modeling the log-odds by a Bayesian linear regression, then we need to map the log-odds to the interval  $[0, 1]$  by the sigmoid function, to make it a valid probability. Specifically, suppose  $a = \mathcal{N}(a; \mu_a, \sigma_a^2)$  and  $y = \sigma(a)$  (note we abuse  $\sigma$  by variances and functions, but it is clear from the context and the subscripts) where  $\sigma(\cdot)$  is a logistic sigmoid function. Then  $y$  has a logistic normal distribution. Given  $p(y)$ , we can make decisions for the value of  $y$ . There are three details that worth noting. First is from the non-linear mapping of  $\sigma(\cdot)$ . One special property of  $p(y)$  is that  $p(y)$  can be bimodal if the base variance or  $\sigma_a$  is large. A consequence is that the mode of  $p(a)$  does not necessarily correspond to  $p(y)$ 's mode and  $\mathbb{E}[y] \neq \sigma(\mathbb{E}[a])$ . Second is for the binary classification: the decision boundary of  $y$ , i.e., 0.5, is consistent with the one of  $x$ , i.e., 0, for decisions either by  $\mathbb{E}[y]$  or by  $\mathbb{E}[a]$ . See Rusmussen & Williams (2005) (Section 3.4) and Bishop et al. (1995) (Section 10.3). Third, if our loss function for decision making is the absolute error, then the best prediction is the median of  $y = \sigma(\hat{a})$  (Friedman et al., 2001) where  $\hat{a}$  is the median of  $a$ . This follows from the monotonicity of  $\sigma(\cdot)$  that does not change the order statistics.

### D.3. Inference over the Change Variable

To infer the posterior distribution of  $s_t$  given observations  $(\mathbf{x}_{1:t}, y_{1:t})$ , we apply Bayes' theorem to infer the posterior log-odds as in the main paper

$$\log \left( \frac{p(s_t = 1 | \mathbf{x}_{1:t}, y_{1:t})}{p(s_t = 0 | \mathbf{x}_{1:t}, y_{1:t})} \right) = \frac{\log(p(\mathbf{x}_t | \mathbf{x}_{1:t-1}, y_{1:t}, s_t = 1))}{\log(p(\mathbf{x}_t | \mathbf{x}_{1:t-1}, y_{1:t}, s_t = 0))} + \xi_0$$

where  $p(\mathbf{x}_t | \mathbf{x}_{1:t-1}, y_{1:t}, s_t)$  is exactly Eq. 11 but has different parameter values dictated by  $s_t$  and  $\beta$ .

In the next part, we show the resulting distribution of the broadening operation.

#### D.3.1. TEMPERING A MULTIVARIATE GAUSSIAN

We will show the tempering operation of a multivariate Gaussian corresponds to multiplying each element in the precision matrix by the fixed temperature, a simple form in the natural space.

Suppose we allow to temper / broaden the  $\theta$ 's multivariate Gaussian distribution before the next time step, accommodating more evidence. Let the broadening constant or temperature be  $\beta \in (0, 1]$ . We derive how  $\beta$  affects the multivariate Gaussian precision.

Write the tempering explicitly,

$$\begin{aligned} p(\boldsymbol{\theta})^\beta &= \frac{1}{Z} \exp \left( -\frac{1}{2} \beta (\boldsymbol{\theta} - \boldsymbol{\mu})^\top \Lambda (\boldsymbol{\theta} - \boldsymbol{\mu}) \right) \\ &= \frac{1}{Z} \exp \left( -\frac{1}{2} (\boldsymbol{\theta} - \boldsymbol{\mu})^\top \Lambda_\beta (\boldsymbol{\theta} - \boldsymbol{\mu}) \right) \end{aligned}$$

among which we are interested in the relationship between  $\Lambda_\beta$  and  $\Lambda$  and  $\beta$ . To this end, re-write the quadratic form in the summation

$$\begin{aligned} &\beta (\boldsymbol{\theta} - \boldsymbol{\mu})^\top \Lambda (\boldsymbol{\theta} - \boldsymbol{\mu}) \\ &= \sum_{i,j} \beta \Lambda_{ij} (\theta_i - \mu_i) (\theta_j - \mu_j) \\ &= \sum_{i,j} \Lambda_{\beta,ij} (\theta_i - \mu_i) (\theta_j - \mu_j) \end{aligned}$$

where we can identify an element-wise relation: for all possible  $i, j$

$$\Lambda_{\beta,ij} = \beta \Lambda_{ij}.$$

#### D.3.2. PREDICTION

As above, we are interested in the posterior predictive distribution for a new test sample  $(\mathbf{x}_*, y_*)$  after absorbing evidence. Let's denote the parameters of  $\theta$ 's posterior distributions by  $\boldsymbol{\mu}_{s_t}$  and  $\Sigma_{s_t}$ , where the dependence over  $s_t$  is made explicit. Since we have two components, this posterior predictive distribution has a mixture form

$$\begin{aligned} p(y_* | \mathbf{x}_*, \mathbf{x}, y) &= p(s_t = 1 | \mathbf{x}, y) p(\mathbf{x}_* | y_*, s_t = 1) + p(s_t = 0 | \mathbf{x}, y) p(\mathbf{x}_* | y_*, s_t = 0) \\ &= p(s_t = 1 | \mathbf{x}, y) \mathcal{N}(y_*; \mathbf{x}_*^\top \boldsymbol{\mu}_{s_t=1}, \sigma_n^2 + \mathbf{x}_*^\top \Sigma_{s_t=1} \mathbf{x}_*) \\ &\quad + p(s_t = 0 | \mathbf{x}, y) \mathcal{N}(y_*; \mathbf{x}_*^\top \boldsymbol{\mu}_{s_t=0}, \sigma_n^2 + \mathbf{x}_*^\top \Sigma_{s_t=0} \mathbf{x}_*) \end{aligned}$$

## E. Visualization of Catastrophic Remembering Effects

In order to demonstrate the effect of catastrophic remembering, we consider a simple linear regression model. We will see that, when the data distribution changes, a Bayesian online learning framework becomes quickly overconfident and unable to adjust to the changing data distribution. On the other hand, with tempering, variational greedy search (VGS) can partially forget the previous knowledge and then adapt to the shifted distribution.



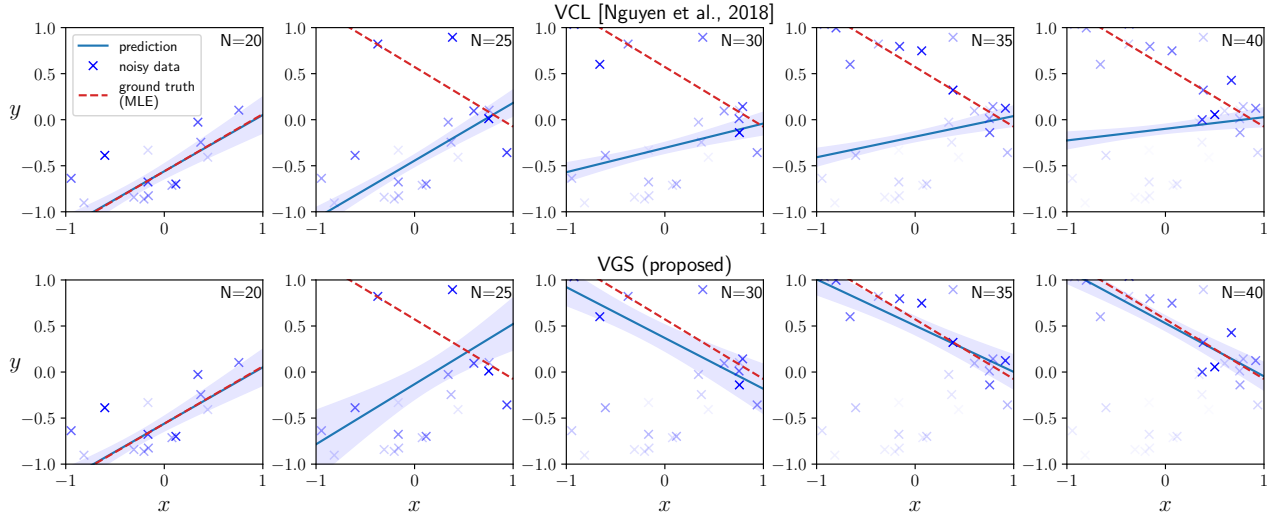


Figure 7. 1D online Bayesian linear regression with distribution shift. More recent samples are colored darker. Due to the catastrophic remembering, VCL fails to adapt to new observations.

**Data Generating Process** We generated the samples by the following generative model:

$$\begin{aligned} x &\sim \text{Unif}(-1, 1), \\ y &\sim \mathcal{N}(f(x), 0.1^2) \end{aligned}$$

where  $f(x)$  equals  $f_1(x) = 0.7x - 0.5$  or  $f_2(x) = -0.7x + 0.5$ . In this experiments, we sampled the first 20 points from  $f_1$  and the remaining 20 points from  $f_2$ .

**Model Parameters** We applied the Bayes updates mentioned in Section D to do inference over the slope and intercept. We set the initial priors of the weights to be standard Gaussian and the observation noise  $\sigma_n^2$  to be the true scale, 0.1. This setting is enough for VCL.

For VGS, we set the same noise variance  $\sigma_n^2 = 0.1$ . For the method-specific parameters, we set  $\xi_0 = \log(0.35/(1 - 0.35))$  and  $\beta = 1/3.5$ .

We plotted the noise-free posterior predictive distribution for both VCL and VGS. That is, let  $f_*(x)$  be the fitted function, we plotted  $p(f_*(x_t)|x_t, \mathcal{D}_{1:t-1}) = \int p(f_*(x_t)|x_t, \mathbf{w}, \mathcal{D}_{1:t-1})p(\mathbf{w}|\mathcal{D}_{1:t-1})d\mathbf{w}$  where  $\mathcal{D}_{1:t-1}$  is the observed samples so far.

**Results** We first visualized the catastrophic remembering effect through a 1D online Bayesian linear regression task where a distribution shift occurred unknown to the regressor (Fig. 7). In this setup, noisy data were sampled from two ground truth functions  $f_1(x) = 0.7x - 0.5$  and  $f_2(x) = -0.7x + 0.5$ , where, with constant additive noise, the first 20 samples came from  $f_1$  and the remaining 20 samples were from  $f_2$ . The observed sample is presented one by one to the regressor. Before the regression starts, the weights (slope and intercept) were initialized to be standard Gaussian distributions. We experimented two different online regression methods, original online Bayesian linear regression (VCL (Nguyen et al., 2018)) and the proposed variational greedy search (VGS). In Fig. 7, to show a practical surrogate for the ground truth, we plotted the maximum likelihood estimation (MLE) for each function given the observations. The blue line and the shaded area correspond to the mean and standard deviation of the posterior predictive distribution after observing  $N$  samples. As shown in Fig. 7, both VCL (top) and VGS (bottom) faithfully fit to  $f_1$  after observing the first 20 samples. However, when another 20 new observations are sampled from  $f_2$ , VCL shows catastrophic remembering of  $f_1$  and cannot adapt to  $f_2$ . VGS, on the other hand, tempers the prior distribution automatically and succeeds in adaptation.

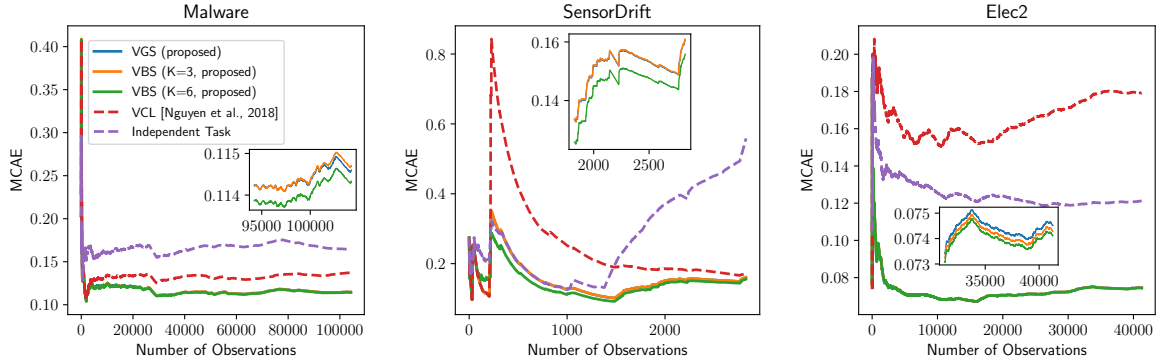


Figure 8. One-step ahead performance of the online malware detection experiments. Proposed methods outperform the baseline.

## F. Experiment Details and Results

In this section, we provide the unstated details of the experiments mentioned in the main paper. These details include but are not limited to hardware infrastructure used to experiment, physical running time, hyperparameter searching, data generating process, evaluation metric, additional results, and so on. The subsection order corresponds to the experiments order in the main paper.

### F.1. An Illustrative Example

**Data Generating Process** To generate Figure 2 in the main paper, we used a step-wise function as ground truth, where the step size was 1 and two step positions were chosen randomly. We sampled 30 equally-spaced points with time spacing 1. To get noisy observations, Gaussian noise with standard deviation 0.5 was added to the points.

**Model Parameters** In this simple one-dimensional model, we used absolute broadening with a Gaussian transition kernel  $K(\mathbf{z}_t, \mathbf{z}'_t) = \mathcal{N}(\mathbf{z}_t - \mathbf{z}'_t, D\Delta t)$  where  $D = 1.0$  and  $\Delta t = 1$ . The inference is thus tractable because  $p(\mathbf{z}_t | s_t)$  is conditional conjugate to  $p(\mathbf{x}_t | \mathbf{z}_t, s_t)$  (and both are Gaussian distributed). We set the prior log-odds  $\epsilon_0$  to  $\log \frac{p(s_t=1)}{p(s_t=0)}$ , where  $p(s_t = 1) = 0.1$ . We used beam size 2 to do the inference.

### F.2. Bayesian Linear Regression Experiments

We performed all linear regression experiments on a laptop with 2.6 GHz Intel Core i5 CPU. All models on SensorDrift and Elec2 dataset finished running within 5 minutes. Running time on Malware dataset varied: VCL and Independent task are within 10 minutes; VGS takes about two and half hours; VBS (K=3) takes about six hours; VBS (K=6) takes about 12 hours. The main difference between VCL’s computation cost and VBS’s computation cost lies in the necessity of inverting the precision matrix into covariance matrix.

**Problem Definitions** We considered both classification experiments (Malware, Elec2) and regression experiments (SensorDrift). The classification datasets have real-value probabilities as targets, permitting to perform regression in log-odds space.

**Setup and Evaluation** We defined each task to consist of a single observation. Models made predictions on the next observation immediately after finishing learning current task. Models were then evaluated with one-step-ahead absolute error<sup>5</sup>, which is then used to compute the mean cumulative absolute error (MCAE) at time  $t$ :  $\frac{1}{t} \sum_{i=1}^t |y_i^* - y_i|$  where  $y^*$  is the predicted value and  $y_i$  is the ground truth. We further approximated the Gaussian posterior distribution by a point mass centered around the mode. It should be noticed that for linear regression, the Laplace Propagation has the same mode as Variational Continual Learning, and the independent task has the same mode as its Bayesian counterpart.

<sup>5</sup>in probability space for classification tasks; in data space for regression tasks

**Results** We reported the result of the dominant hypothesis of VBS with large beam size. Fig. F.2 shows MCAE over time for all three datasets. Our methods remain lower prediction error of all time while baselines are subject to strong fluctuations or inability to adapt to distribution shifts. Another observation is that VBS with different beam sizes performed similarly in this case.

### F.2.1. MALWARE<sup>6</sup>

**Dataset** There are 107856 programs collected from 2010.11 to 2014.7 in the monthly order. Each program has 482 counting features and a real-valued probability  $p \in [0, 1]$  of being malware. This ground truth probability is the proportion of 52 antivirus solutions that label malware. We used the first-month data (2010.11) as the validation dataset and the remaining data as the test dataset. To enable analytic online update, we cast the binary classification problem in the log-odds space and performed Bayesian linear regression. We filled log-odds boundary values to be  $-5$  and  $4$ , corresponding to probability 0 and 1, respectively. Our methods achieved comparable results reported in (Huynh et al., 2017) on this dataset.

**Hyperparameters** We searched the hyperparameters  $\sigma_n^2, \xi_0 = \log \frac{p_0}{1-p_0}$ , and  $\beta$  using the validation set. Specifically, we extensively searched  $\sigma_n^2 \in \{0.1, 0.2, \dots, 0.9, 1, 2, \dots, 10, 20, \dots, 100\}$ ,  $p_0 \in \{0.5\}$ ,  $\beta^{-1} \in \{1.01, 1.05, 1.1, 1.2, 1.5, 2, 5\}$ . On most values the optimization landscape is monotonic and thus the search quickly converges around a local optimizer. Within the local optimizer, we performed the grid search, which focused on  $\beta \in [1.05, 1.2]$ .

We found all methods favored  $\sigma_n^2 = 40$ . And for VGS and VBS, the uninformative prior of the change variable  $p_0 = 0.5$  was already a suitable one. VGS selected  $\beta^{-1} = 1.2$ , VBS (K=3) selected  $\beta^{-1} = 1.07$ , and VBS (K=6) selected  $\beta^{-1} = 1.05$ . Although searched  $\beta^{-1}$  varies for different beam size, the performance of different beam size in this case, based on our experience, is insensitive to the varying  $\beta$ .

### F.2.2. SENSORDRIFT<sup>7</sup>

**Dataset** We focused on one kind of gas, *Acetaldehyde*, retrieved from the original gas sensor drift dataset (Vergara et al., 2012), which spans 36 months. We formulated a regression problem of predicting the gas concentration level given all the other features. The dataset contains 128 features and 2926 samples in total. We used the first batch data (in the original dataset) as the validation set and the others as the test set. Since the scales of the features vary greatly, we scaled each feature with the sample statistics computed from the validation set, leading to zero mean and unit standard deviation for each feature.

**Hyperparameters** Since we scaled the dataset, we therefore set the hyperparameter  $\sigma_n^2 = 1$  for all methods. We searched  $\xi_0 = \log \frac{p_0}{1-p_0}$  and  $\beta$  using the validation set. Specifically, we searched a larger range of  $\beta^{-1} \in \{1.05, 1.1, 1.2, 1.5, 2, 5, 10, 100, 1000\}$  and finer resolution of  $p_0 \in \{0.5 + k \times 1e-5, k \in \mathbb{Z}\}$  than the other two datasets.

All methods favored  $\beta^{-1} = 100$ . For  $p_0$ , VGS favored  $p_0 = 0.50001$ ; VBS (K=3) selected  $p_0 = 0.5003$ ; and VBS (K=6) selected  $p_0 = 0.50071$ .

### F.2.3. ELEC2<sup>8</sup>

**Dataset** The dataset contains the electricity price over three years of two Australian states, New South Wales and Victoria (Harries & Wales, 1999). While the original problem was 0-1 binary classification, we re-produced the targets with real-value probabilities since all necessary information forming the original target is contained in the dataset. Specifically, we re-defined the target to be the probability of the price in New South Wales increasing relative to the price of the last 24 hours. Then we performed linear regression in the log-odds space. We filled log-odds boundary values to be  $-4$  and  $4$ , corresponding to probability 0 and 1, respectively. After removing the first 48 samples (for which we cannot re-produce the targets), we had 45263 samples, and each sample comprised 14 features. The first 4000 samples were used for validation while the others were used for test.

<sup>6</sup><https://archive.ics.uci.edu/ml/datasets/Dynamic+Features+of+VirusShare+Executables>

<sup>7</sup><http://archive.ics.uci.edu/ml/datasets/Gas+Sensor+Array+Drift+Dataset+at+Different+Concentrations>

<sup>8</sup><https://www.openml.org/d/151>

Table 2. Convolution Neural Network Architecture

LAYER	FILTER SIZE	FILTERS	STRIDE	ACTIVATION	DROPOUT
CONVOLUTIONAL	$3 \times 3$	32	1	ReLU	
CONVOLUTIONAL	$3 \times 3$	32	1	ReLU	
MAXPOOLING	$2 \times 2$		2		0.2
CONVOLUTIONAL	$3 \times 3$	64	1	ReLU	
CONVOLUTIONAL	$3 \times 3$	64	1	ReLU	
MAXPOOLING	$2 \times 2$		2		0.2
FULLYCONNECTED		10		SOFTMAX	

Table 3. Hyperparameters of Bayesian Deep Learning Models for CIFAR-10

MODEL	LEARNING RATE	BATCH SIZE	NUMBER OF EPOCHS	$\beta$	$\xi_0$	$T$
LP	0.001	64	150	N/A	N/A	N/A
VCL	0.0005	64	150	N/A	N/A	N/A
VBS	0.0005	64	150	2/3	0	20000

**Hyperparameters** We searched the hyperparameters  $\sigma_n^2, \xi_0 = \log \frac{p_0}{1-p_0}$ , and  $\beta$  using the validation set. Specifically, we extensively searched  $\sigma_n^2 \in \{0.01, 0.02, \dots, 0.1, 0.2, \dots, 1, 2, \dots, 10, 20, \dots, 100\}$ ,  $p_0 \in \{0.5\}$ ,  $\beta^{-1} \in \{1.05, 1.1, 1.2, 1.5, 2, 5\}$ .

VCL favored  $\sigma_n^2 = 0.01$ , and we set this value for all other methods. VGS selected  $\beta^{-1} = 1.2$ . VBS (K=3) and VBS (K=6) inherited the same  $\beta$  value from VGS.

### F.3. Bayesian Deep Learning Experiments

We performed the Bayesian Deep Learning experiments on a server with Intel(R) Xeon(R) Gold 5218 CPU @ 2.30GHz and Nvidia TITAN RTX GPUs. Regarding the running time, VCL, and Independent task (Bayes) takes five hours to finish training; Independent task takes three hours; VGS takes two GPUs and five hours; VBS (K=3) takes six GPUs and five hours; VBS (K=6) takes six GPUs and 10 hours. When utilizing multiple GPUs, we implemented task multiprocessing with process-based parallelism.

**Transformations** We used Albuementations (Buslaev et al., 2020) to implement the transformations as covariate shifts. As stated in the main paper, the transformation involved rotation, scaling, and translation. Each transformation factor followed a fixed distribution: rotation degree conformed to  $\mathcal{N}(0, 10^2)$ ; scaling limit conformed to  $\mathcal{N}(0, 0.3^2)$ ; and the magnitude of vertical and horizontal translation limit conformed to Beta(1, 10), and the sampled magnitude is then rendered positive or negative with equal probability. The final scaling and translation factor should be the corresponding sampled limit plus 1, respectively.

**Neural Network Architecture** We used the same convolutional neural network architecture for both datasets, which can be found in Table 2. We implemented the Bayesian models using TensorFlow Probability and the non-Bayesian counterpart (namely Laplace Propagation) using TensorFlow Keras. Every bias term in all the models were treated deterministically and were not affected by any regularization.

Table 4. Hyperparameters of Bayesian Deep Learning Models for SVHN.

MODEL	LEARNING RATE	BATCH SIZE	NUMBER OF EPOCHS	$\beta$	$\xi_0$	$T$
LP	0.001	64	150	N/A	N/A	N/A
VCL	0.00025	64	150	N/A	N/A	N/A
VBS	0.00025	64	150	2/3	0	20000

**Tempered Conditional ELBO** In the presence of massive observations and a large neural network, posterior distributions of change variables usually have very low entropy because of the very large magnitude of the difference between conditional ELBOs as in Eq. 7. Therefore change variables become over confident about the switch-state decisions. The situation gets even more severe in beam search settings where almost all probability mass is centered around the most likely hypothesis while the other hypotheses get little probability and thereby will not take effect in predictions. A possible solution is to temper the conditional ELBO (or the marginal likelihood) and introduce more uncertainty into the change variables. To this end, we divide the conditional ELBO by the number of observations. It is equivalent to set  $T = 20000$  in Eq. 7. This practice renders every hypothesis effective in beam search setting.

**Hyperparameters, Initialization, and Model Training** The hyperparameters used across all of the models for the different datasets are listed in Tables 3 and 4. Regarding the model-specific parameters, we set  $\xi_0$  to 0 for both datasets and searched  $\beta$  in the values  $\{5/6, 2/3, 1/2, 1/4\}$  on a validation set. We used the first 5000 images in the original test set as the validation set, and the others as the test set. We found that  $\beta = 2/3$  performs relatively well for both data sets. Optimization parameters, including learning rate, batch size, and number of epochs, were selected to have the best validation performance of the classifier on one independent task. To estimate the change variable  $s_t$ 's variational parameter, we approximated the conditional ELBOs 4 by averaging 10000 Monte Carlo samples.

As outlined in the main paper, we initialized each algorithm by training the model on the full, untransformed dataset. The model weights used a standard Gaussian distribution as the prior for this meta-initialization step.

When optimizing with variational inference, we initialized  $q(\mathbf{z}_t)$  to be a point mass around zero for stability. When performing non-Bayesian optimization, we initialized the weights using Glorot Uniform initializer (Glorot & Bengio, 2010). All bias terms were initialized to be zero.

We performed both the Bayesian and non-Bayesian optimization using ADAM (Kingma & Ba, 2014). For additional parameters of the ADAM optimizer, we set  $\beta_1 = 0.9$  and  $\beta_2 = 0.999$  for both data sets. For the deep Bayesian models specifically, which include VCL and VBS, we used stochastic black box variational inference (Ranganath et al., 2014; Kingma & Welling, 2013; Zhang et al., 2018). We also used the Flipout estimator (Wen et al., 2018) to reduce variance in the gradient estimator.

**Predictive Distributions** We evaluated the ensemble predictive posterior distribution of the test set by the following approximation:

$$p(\mathbf{y}_t|\mathbf{x}_t, \mathcal{D}_{1:t}) \approx \frac{1}{S} \sum_{k=1}^K \sum_{s=1}^S w_k p(\mathbf{y}_t|\mathbf{x}_t, \mathbf{z}_{t,k}^{(s)})$$

where  $K$  is the beam size,  $w_k$  is the normalized weight of the  $k^{\text{th}}$  hypothesis after truncation, and  $S$  is the number of Monte Carlo samples from the variational posterior distribution  $q_t(\mathbf{z}_t)$ . The most likely hypothesis evaluation alters  $w_k$  such that all probability mass centers around the mode. In our experiments we found  $S = 10$  to be sufficient. We take  $\arg \max_{\mathbf{y}_t} p(\mathbf{y}_t|\mathbf{x}_t, \mathcal{D}_{1:t})$  to be the predicted class.

VGS and VCL set  $K = 1$  for the single hypothesis in the above formula. LP further only used the MAP estimation  $\mathbf{z}_t^*$  to predict the test set:  $p(\mathbf{y}_t|\mathbf{x}_t, \mathcal{D}_{1:t}) \approx p(\mathbf{y}_t|\mathbf{x}_t, \mathbf{z}_t^*)$ .

**Standard Deviation in the Main Text Table 1** The results in this table were summarized and reported by taking the average over tasks. Each algorithm's confidence, which is usually evaluated by computing the standard deviation across tasks in stationary environments, now is hard to evaluate due to the non-stationary setup. These temporal image transformations will largely affect the performance, leaving the blindly computed standard deviation meaningless since the standard deviation across all tasks represents both the data transformation variation and the modeling variation. To evaluate the algorithm's confidence, we proposed a three-stage computation. We first segment the obtained performance based on the image transformations (in our case, we separate the performance sequence every three tasks). Then we compute the standard deviation for every performance segment. Finally, we average these standard deviations across segments as the final one to be reported. In this way, we can better account for the data variation in order to isolate the modeling variation.

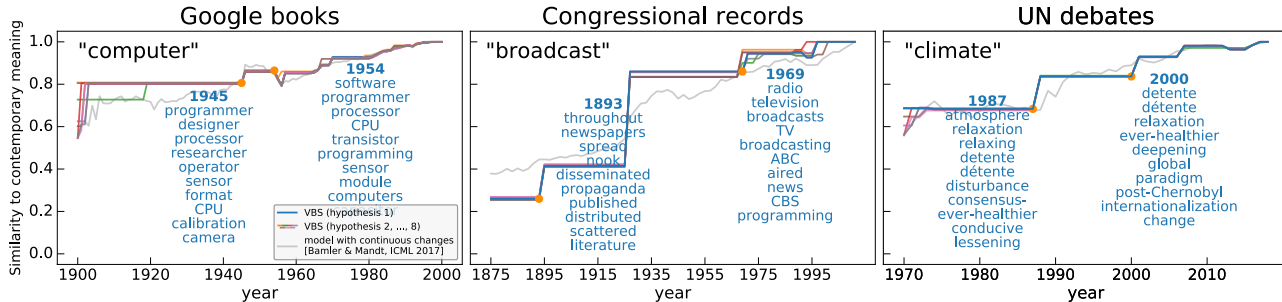


Figure 9. Additional results of Dynamic Word Embeddings on Google books, Congressional records, and UN debates.

Table 5. Hyperparameters of Dynamic Word Embedding Models

CORPUS	VOCAB	DIMS	$\beta$	LEARNING RATE	EPOCHES	$\xi_0$	BEAM SIZE (K)	$T$
GOOGLE BOOKS	30000	100	0.5	0.01	5000	-10	8	1
CONGRESSIONAL RECORDS	30000	100	0.5	0.01	5000	-10	8	1
UN DEBATES	30000	20	0.25	0.01	5000	-1	8	1

#### E.4. Dynamic Word Embeddings Experiments

We performed the Dynamic Word Embeddings experiments on a server with Intel(R) Xeon(R) Gold 5218 CPU @ 2.30GHz and Nvidia TITAN RTX GPUs. Regarding the running time, for qualitative experiments, Google Books and Congressional Records take eight GPUs and about 24 hours to finish; UN Debates take eight GPUs and about 13 hours to finish. For quantitative experiments, since the vocabulary size and latent dimensions are smaller, each model corresponding to a specific  $\xi_0$  takes eight GPUs and about one hour to finish. When utilizing multiple GPUs, we implemented task multiprocessing with process-based parallelism.

**Data and Preprocessing** All datasets, Congressional Records<sup>9</sup>, UN General Debates<sup>10</sup>, and Google Books<sup>11</sup> can be downloaded online.

We tokenized Congressional Records and UN General Debates with pre-trained Punkt tokenizer in NLTK<sup>12</sup>. We constructed the co-occurrence matrices with a moving window of size 10 centered around each word. Google books are already in Ngram format.

**Model Assumptions** As outlined in the main paper, we analyzed the semantic changes of individual words over time. We augmented the probabilistic models proposed by Bamler & Mandt (2017) with the spike and slab novelty prior (Eq. 3 in the main paper) to encourage temporal sparsity. We pre-trained the *context* word embeddings<sup>13</sup> using the whole corpus, and kept them constant when updating the *target* word embeddings. This practice denied possible interference on one target word embedding from the updates of the others. If we did not employ this practice, the spike and slab prior on word  $i$  would

<sup>9</sup>[https://data.stanford.edu/congress\\_text](https://data.stanford.edu/congress_text)

<sup>10</sup><https://dataverse.harvard.edu/dataset.xhtml?persistentId=doi:10.7910/DVN/0TJX8Y>

<sup>11</sup><http://storage.googleapis.com/books/ngrams/books/datasetsv2.html>

<sup>12</sup><https://www.nltk.org/>

<sup>13</sup>We refer readers to (Mikolov et al., 2013; Bamler & Mandt, 2017) for the difference between target and context word embeddings.

Table 6.  $\xi_0$  of Document Dating Tasks

CORPUS	$\xi_0$
GOOGLE BOOKS	-1000000, -100000, -5120, -1280, -40
CONGRESSIONAL RECORDS	-100000, -1280, -320, -40
UN DEBATES	-128, -64, -32, -4

lead to two branches of the “remaining vocabulary” (embeddings of the remaining words in the vocabulary), conditioned either on the spike prior of word  $i$  or on the slab prior. This hypothetical situation gets severe when every word in the vocabulary can take two different priors, thus leading to exponential branching of the sequences of inferred change points. When this interference is allowed, the exponential scaling of hypotheses translates into exponential scaling of possible word embeddings for a single target word, which is not feasible to compute for any meaningful vocabulary sizes and number of time steps. To this end, while using a fixed, pre-trained context word embeddings induces a slight drop of predictive performance, the computational efficiency improves tremendously and the model can actually be learned.

**Hyperparameters and Optimization** Qualitative results in Figure 4 in the main paper were generated using the hyperparameters in Table 5. The initial prior distribution used for all latent embedding dimensions was a standard Gaussian distribution. We also initialized all variational distributions with standard Gaussian distributions. For model-specific hyperparameters  $\beta$  and  $\xi_0$ , we first searched the broadening constant  $\beta$  to have the desired jump magnitude observed from the semantic trajectories mainly for medium-frequency words. We then tuned the bias term  $\xi_0$  to have the desired change frequencies in general. We did the searching for the first several time steps. We performed the optimization using black box variational inference and ADAM. For additional parameters of ADAM optimizer, we set  $\beta_1 = 0.9$  and  $\beta_2 = 0.999$  for all three corpora. In this case, we did **not** temper the conditional ELBO by the number of observations.

Quantitative results of VGS in Figure 5 in the main paper were generated by setting a smaller vocabulary size and embedding dimension, 10,000 and 20, respectively for all three corpora. We used an eight-hypothesis (K=8) VBS to perform the experiments. Other hyperparameters were inherited from the qualitative experiments except  $\xi_0$ , whose values used to form the rate-distortion curve can be found in Table 6. We enhanced beam diversification by dropping the bottom two hypotheses instead of the bottom third hypotheses before ranking. On the other hand, the baseline, “binning”, had closed-form performance if we assume (i) a uniformly distributed year in which a document query is generated, (ii) “binning” perfectly locates the ground truth episode, and (iii) the dating result is uniformed distributed within the ground truth episode. The  $L1$  error associated with “binning” with episode length  $L$  is  $\mathbb{E}_{t \sim \mathcal{U}(1,L), t' \sim \mathcal{U}(1,L)} [|t - t'|] = \frac{L-1}{2}$ . By varying  $L$ , we get binning’s rate-distortion curve in Figure 5 in the main paper.

**Additional Results** Additional qualitative results can be found in Figure 9. it, again, reveals interpretable semantic changes of each word: the first change of “computer” happens in 1940s—when modern computers appeared; “broadcast” adopts its major change shortly after the first commercial radio stations were established in 1920; “climate” changes its meaning at the time when Intergovernmental Panel on Climate Change (IPCC) was set up, and when it released the assessment reports to address the implications and potential risks of climate changes.

**Predictive Distributions** In the demonstration of the quantitative results, i.e., the document dating experiments, we predicted the year in which each held-out document’s word-word co-occurrence statistics  $\mathbf{x}$  have the highest likelihood and measured  $L1$  error. To be specific, for a given document in year  $t$ , we approximated its likelihood under year  $t'$  by evaluating  $\frac{1}{|V|} \log p(\mathbf{x}_t | \mathbf{z}_{t'}^*)$ , where  $\mathbf{z}_{t'}^*$  is the mode embedding in year  $t'$  and  $|V|$  is the vocabulary size. We predicted the year  $t^* = \arg \max_{t'} \frac{1}{|V|} \log p(\mathbf{x}_t | \mathbf{z}_{t'}^*)$ . We then measured the  $L1$  error by  $\frac{1}{T} \sum_i |t_i - t_i^*|$  given  $T$  truth-prediction pairs.